

1
2 Structural characteristics and Re-Os dating of quartz-pyrite veins in the
3 Lewisian Gneiss Complex, NW Scotland: evidence of an Early
4 Paleoproterozoic hydrothermal regime during terrane amalgamation.

5
6 R. Vernon^{1*}, R.E. Holdsworth^{1†}, D. Selby¹, E. Dempsey¹, A. J. Finlay¹ & A. E. Fallick²

7
8 ¹ *Department of Earth Sciences, Durham University, Durham, DH1 3LE, UK.*

9 ² *SUERC, Scottish Enterprise Technology Park, Rankine Avenue, East Kilbride, G75 0QF,*
10 *UK.*

11 **Current address: Department of Geology, University of Leicester, University Road,*
12 *Leicester, LE1 7RH, UK.*

13 [†]Corresponding author

14
15 **Abstract:** In the Archaean basement rocks of the Assynt and Gruinard terranes of the
16 mainland Lewisian Complex in NW Scotland, a regional suite of quartz-pyrite veins cross-cut
17 regional Palaeoproterozoic (Badcallian, ca. 2700 Ma; Inverian, ca. 2480 Ma) fabrics and
18 associated Scourie dykes. The quartz veins are overprinted by amphibolite-greenschist
19 facies Laxfordian deformation fabrics (ca. 1760 Ma) and later brittle faults. The hydrothermal
20 mineral veins comprise a multimodal system of tensile/hybrid hydraulic fractures which are
21 inferred to have formed during a regional phase of NW-SE extension. The almost orthogonal
22 orientation of the quartz veins (NE-SW) to the Scourie dykes (NW-SE) are incompatible and
23 must result from distinct paleostress regimes suggesting they are related to different tectonic
24 events. This hypothesis is supported by Rhenium-Osmium dating of pyrite that yields an age
25 of 2249 ± 77 Ma, placing the vein-hosted mineralisation event after the oldest published
26 dates for the Scourie Dykes (2420 Ma), but before the youngest ages (1990 Ma). Sulphur
27 isotope analysis suggests that the sulphur associated with the pyrite is isotopically

1
2 28 indistinguishable from primitive mantle. The presence of the ca. 2250 Ma quartz-pyrite veins
3
4 29 in both the Assynt and Gruinard terranes confirms that these crustal units were
5
6 30 amalgamated during or prior to Inverian deformation. The absence of the veins in the
7
8 31 Rhiconich Terrane is consistent with the suggestion that it was not finally amalgamated to
9
10 32 the Assynt Terrane until the Laxfordian.

11 33 **[End]**
12
13
14
15
16
17
18
19
20
21
22
23
24
25
26
27
28
29
30
31
32
33
34
35
36
37
38
39
40
41
42
43
44
45
46
47
48
49
50
51
52
53
54
55
56
57
58
59
60
61
62
63
64
65

34 1. Introduction

1
2 35 The Archaean gneisses of the Lewisian Complex in NW Scotland form a well exposed and
3
4 36 relatively accessible area of Laurentian continental basement rocks that lie in the immediate
5
6 37 foreland region of the Palaeozoic Caledonian Orogen (Fig. 1). Like many regions of
7
8 38 continental metamorphic basement, the Lewisian Complex preserves evidence for multiple
9
10 39 episodes of igneous intrusion, ductile and brittle deformation together with associated
11
12 40 phases of metamorphism and mineralisation (e.g. Sutton and Watson 1951; Park 1970;
13
14 41 Beacom et al., 2001; Wheeler et al., 2010). Whilst cross-cutting and overprinting
15
16 42 relationships observed in the field and thin section allow *relative* age relationships to be
17
18 43 established on both regional and local scales, only radiometric ages are able to give
19
20 44 information concerning the absolute timing of events. Despite the emergence of an
21
22 45 increasing number of geochronometers for Earth Scientists, an enduring problem in many
23
24 46 basement regions is a relative paucity of material suitable for reliable radiometric dating. This
25
26 47 lack of absolute age determinations has become a particularly significant problem in the
27
28 48 Lewisian Complex since Kinny et al. (2005) and Friend and Kinny (2001) proposed that the
29
30 49 Lewisian may comprise a number of lithologically and geochronologically distinct tectonic
31
32 50 units or terranes assembled progressively during a series of Precambrian amalgamation
33
34 51 episodes perhaps spanning more than a billion years (see Park, 2005; Goodenough et al.,
35
36 52 2013 for discussions).

37
38 53 This paper describes the lithology, field relationships and microstructures of a little
39
40 54 described set of quartz-pyrite veins that are recognised throughout the Assynt Terrane and
41
42 55 within the Gruinard Terrane. These mineralised hydrofractures display a consistent set of
43
44 56 contact relationships relative to regionally recognised igneous, metamorphic and
45
46 57 deformational events. Rhenium-osmium (Re-Os) geochronology on pyrites collected from
47
48 58 these veins is used to obtain a consistent set of ages that better constrain the absolute
49
50 59 timing of events in this important part of the Lewisian Complex in NW Scotland. It also
51
52 60 illustrates the potential value of the Re-Os technique as a means of dating sulphide
53
54 61 mineralisation events in geologically complex continental basement terrains worldwide.
55
56
57
58
59
60
61
62
63
64
65

62

63 2. Regional Setting

64 The Precambrian rocks of the Lewisian Complex of NW Scotland form a fragment of the
65 continental basement of Laurentia that lies to the west of the Caledonian Moine Thrust (Fig.
66 1). The rocks are for the most part little affected by Caledonian deformation and have
67 experienced a number of major crustal-scale geological events during the Archaean and
68 Palaeoproterozoic. The Lewisian Complex is divided into a number of tectonic regions or
69 terranes which are predominantly separated by steeply-dipping shear zones or faults (e.g.
70 Park et al., 2002; Park, 2005).

71 The Assynt Terrane (Fig. 1) forms the central part of the Lewisian Complex in
72 mainland NW Scotland. It comprises grey, banded, tonalite-trondjemite-granodioritic (TTG)
73 gneisses which are locally highly heterogeneous lithologically, ranging from ultramafic to
74 acidic compositions (e.g., Sheraton et al., 1973). The TTG gneisses are thought to be
75 derived from igneous plutons intruded at 3030 to 2960 Ma (high precision U-Pb and Sm-Nd
76 geochronology; Hamilton et al., 1979; Friend and Kinny, 1995; Kinny and Friend, 1997).
77 These rocks then underwent deformation and granulite-facies metamorphism during the so-
78 called Badcallian event(s) which led to significant depletion of large-ion lithophile elements in
79 the TTG gneisses that is more extensive in the Assynt Terrane compared to adjacent
80 amphibolite-facies terranes (e.g. Rhiconich, Gruinard; Moorbath et al., 1969; Cameron,
81 1994; Wheeler et al., 2010). The timing of Badcallian events are incompletely resolved with
82 current age constraints suggesting either *ca.* 2760 Ma (e.g., Corfu et al.1994; Zhu et al.,
83 1997), and/or *ca.* 2490 - 2480 Ma (e.g., Friend and Kinny 1995; Kinny & Friend, 1997).

84 The central part of the Assynt Terrane is cut by the major NW-SE-trending, steeply
85 dipping dextral transpressional Canisp Shear Zone (CSZ) which has a maximum width of
86 1.5km (Attfield, 1987; Fig. 1). There are also many other smaller steeply-dipping, NW-SE to
87 WNW-ESE trending minor shear zones cutting the surrounding Badcallian gneisses (Park
88 and Tarney, 1987). Some of these shear zones, including the CSZ, developed initially during
89 Inverian deformation and amphibolites-facies retrogression which affected substantial parts

90 of the Assynt Terrane. The absolute age of this event is the subject of significant uncertainty
91 and debate, with a majority of studies considering it to be *ca.* 2490 - 2480 Ma (e.g., Corfu et
92 al. 1994; Love et al., 2004; Goodenough et al., 2013). Others (e.g., Friend and Kinny 1995;
93 Kinny and Friend, 1997) suggest that the Inverian is a younger – as yet undated – event
94 younger than *ca.* 2480 Ma while still pre-dating the oldest Scourie dykes. These mafic to
95 ultramafic Scourie dykes are found throughout the Assynt Terrane, ranging in thickness from
96 a few mm to several tens of m and were intruded *ca.* 1900 - 2400 Ma (Rb-Sr whole rock and
97 U-Pb geochronology; Chapman 1979; Heaman & Tarney, 1989; Davies & Heaman 2014).
98 The NW-SE-trending Scourie dykes cross-cut local Inverian fabrics and display evidence of
99 having been emplaced under amphibolite facies pressures and temperatures, i.e. in the
100 middle crust, possibly immediately following the Inverian event (O'Hara, 1961; Tarney, 1973;
101 Wheeler et al., 2010).

102 In the Assynt Terrane, the significantly later main phase Laxfordian event has
103 traditionally been associated with the shearing of the Scourie dykes and widespread
104 retrogression of the TTG gneisses under lower amphibolite to upper greenschist-facies
105 metamorphic conditions (e.g., Sutton and Watson, 1951; Attfield, 1987; Beacom et al.,
106 2001). The Laxfordian is recognised throughout much of the Lewisian complex and appears
107 to be a long lived series of events starting with a series of magmatic events *ca.* 1900-1870
108 Ma – at least some of which are related to island arc development – followed by a protracted
109 orogenic episode lasting from 1790 - 1660 Ma (see discussion in Goodenough et al., 2013).
110 The effects of Laxfordian reworking in the Assynt Terrane are highly localised, being largely
111 restricted to the central part (*ca.* 1km wide) of the CSZ and other shear zones, as well as
112 along the margins of the Scourie dykes. This contrasts with the neighbouring Rhiconich and
113 Gruinard Terranes where the Laxfordian event reached amphibolite facies and was
114 associated with more pervasive ductile shearing and reworking (Droop et al., 1989). This has
115 led to the suggestion that the Assynt Terrane represents a shallower depth crustal block
116 during the Laxfordian (e.g., Dickinson and Watson, 1976; Coward and Park, 1987).

117 In the Assynt and Grunard terranes, a younger set of 'late Laxfordian' sinistral low
118 greenschist-facies mylonitic shear zones, brittle faults and localized folds is recognised
119 developed sub-parallel to the pre-existing high-strain fabrics in Laxfordian and Inverian shear
120 zones (see Beacom et al. 2001). These structures include the Loch Assynt Fault (Fig. 1).
121 The precise age of the 'late-Laxfordian' faulting is poorly constrained, but these structures
122 are unconformably overlain by the unmetamorphosed and little deformed *ca.* 1200 Ma
123 Torridonian Stoer Group. This suggests that the presently exposed parts of the Lewisian
124 Complex had been exhumed to the surface by *ca.* 1200 Ma. Regionally, both the Stoer
125 Group and the Lewisian Complex are unconformably overlain by younger Torridonian
126 sequences (Diabeg and Torridon groups) thought to have been deposited no earlier than 1.1
127 Ga (Park et al. 1994).

128

129 *Lewisian host rocks*

130 The Badcallian amphibolite- to granulite-facies TTG gneisses of the Assynt Terrane show
131 foliation development on all scales (e.g., Fig 2a), from millimetres to tens of metres (e.g.
132 Sheraton et al., 1973). The foliation is best developed in intermediate composition gneisses,
133 where it is defined by 0.5 to 5 cm thick layers of contrasting light (plagioclase and quartz)
134 and dark (pyroxene, hornblende and biotite) layers, with individual layers rarely continuing
135 for more than a few metres (Jensen, 1984). Representative samples from the Loch Assynt
136 area typically contain 30% quartz, 20% plagioclase, 10% microcline, 10% orthopyroxene and
137 30% heavily retrogressed clinopyroxene. Relict grains of the latter mineral are replaced by
138 fine grained intergrown aggregates of chlorite, epidote, actinolite and hornblende.

139 The Badcallian gneisses were reworked in dextral-reverse shear zones (e.g., the
140 CSZ) during the Inverian, which imposed a NW-SE foliation in the rocks, mainly by
141 reorientation and attenuation of the pre-existing gneissose foliation (e.g., Fig. 2b; Attfield,
142 1987). Deformation within the Inverian shear zones is extremely heterogeneous, with lenses
143 of lower-strain, more massive material enclosed by anastomosing bands of highly deformed,
144 sheared gneiss (e.g., Attfield, 1987; Chattopadhyay et al., 2010). Representative samples of

145 reworked Inverian gneisses from within the CSZ contain 20% quartz, 40% feldspar
146 (predominantly plagioclase with alteration bands), 5% pyroxene, 15% hornblende, 15%
147 biotite and chlorite, and 5% other minerals such as epidote. The hornblende, epidote, biotite
148 and chlorite are likely to be a product of the breakdown and hydration of pyroxenes during
149 retrogression (Beach, 1976). The quartz crystals contain 0.25 - 1mm subgrains and form
150 irregular, sub-parallel ribbons of crystals, which are smaller than in the undeformed
151 Badcallian gneisses, possibly due to syn-tectonic recrystallisation (Jensen, 1984).

152 The Laxfordian event reactivated the central part of the CSZ with a dextral shear
153 sense, producing a new, finer foliation (e.g., Fig. 2d; Sheraton et al., 1973; Attfeld, 1978).
154 Commonly, the reworked rocks in both small and large shear zones have a mineralogy that
155 differs significantly from that of the original gneiss and the extent of the changes that occur
156 appears to be in proportion to the intensity of the deformation (e.g., see Beach, 1976). A
157 typical sample of Laxfordian-deformed gneiss from the CSZ contains 75% quartz, 10%
158 hornblende, 10% biotite and muscovite, and 5% feldspar porphyroblasts (typically ~1mm in
159 size). The quartz is banded on a millimetre scale with alternating bands of small quartz
160 grains (<100 μ m) and larger quartz grains (~500 μ m to 1mm) which form an anastomosing
161 schistose foliation (Jensen, 1984). Quartz grain boundaries are often pinned by aligned
162 micas and layers richer in mica therefore tend to show finer quartz grain sizes compared to
163 mica-poor layers. The quartz crystals themselves are often elongate and contain poorly
164 developed subgrains. Petrographic observations of Lewisian gneisses show that during
165 regression, pyroxene is first replaced by hornblende which is then replaced by biotite in the
166 most intensely deformed gneisses (Beach, 1976). The Laxfordian reworking occurred in
167 intense zones which anastomose around relict lenses of Badcallian or Inverian gneiss
168 (Sheraton et al., 1973). Tight intrafolial folds are common within the Laxfordian-deformed
169 gneisses and, in places, Inverian folds have been refolded (e.g. on the coast at Port Alltan
170 na Bradhan; see Attfeld, 1987; Chattopadhyay et al., 2010). The Scourie dykes within and
171 adjacent to the CSZ have also been pervasively affected by Laxfordian reworking with

172 shearing particularly concentrated along their margins (Sheraton et al., 1973). Most dykes in
173 the CSZ are sheared into near concordance with the surrounding foliation in the gneisses.

174

175 **3. Field and Laboratory Methods**

176 *3.1. Fieldwork*

177 Fieldwork was carried out visiting well-exposed examples of quartz-pyrite vein localities in
178 the Assynt Terrane and in one area of the Gruinard Terrane (Fig. 1). The relative ages of
179 country rock fabrics and veins were determined at 83 locations using cross-cutting
180 relationships and the orientations of both veins and fabrics were measured. Representative
181 (orientated) hand samples of both country rocks and veins were taken at a number of key
182 localities in order to study deformation microstructures using an optical microscope and also
183 to extract fresh samples of pyrite for Re-Os dating. Having separated appropriate material
184 for dating, we used Re-Os geochronology to determine the age of sulphide (pyrite)
185 mineralization present in several of the quartz veins. We additionally determined sulphur
186 isotope compositions of the dated samples to yield evidence of the origin of the sulphur and
187 by inference the hydrothermal fluids associated with the quartz-pyrite vein formation.

188

189 *3.2. Rhenium-Osmium Geochronology Analytical Methods*

190 Six pyrite samples co-genetic with quartz veining were analyzed for their rhenium (Re) and
191 osmium (Os) abundances and isotopic compositions. The analyses were conducted at the
192 TOTAL Laboratory for Source Rock Geochronology and Geochemistry at Durham
193 University. The pyrite sample set was collected from five locations: four in the Assynt
194 Terrane and one in the Gruinard Terrane (Fig. 1; Table 1).

195 The pyrite samples were isolated from the vein host material by crushing, without
196 metal contact, to a < 5 mm grain size. After this stage > 1 g of pyrite was separated from the
197 crushed vein by hand picking under a microscope to obtain a clean mineral separate. The
198 Re and Os analysis reported in this study followed the analytical protocols of Selby et al.
199 (2009). In brief, this involved loading ~ 0.4 g of accurately weighed pyrite into a carius tube

200 with a known amount of a ^{185}Re and ^{190}Os tracer (spike) solution and 11 ml of inverse *aqua*
201 *regia* (3 ml 11N HCl and 8 ml 15 N HNO_3). The carius tubes were then sealed and placed in
202 an oven at 220°C for 48 hrs. Osmium was isolated and purified from the acid medium using
203 CHCl_3 solvent extraction and micro-distillation, with Re separated by anion exchange column
204 and single-bead chromatography. The Re and Os fractions were then loaded onto Ni and Pt
205 filaments, respectively, and analyzed for their isotope compositions using negative-ion mass
206 spectrometry on a Thermo Electron TRITON mass spectrometer. Rhenium isotopes were
207 measured statically using Faraday Collectors, with the Os measured in peak hopping mode
208 using the Secondary Electron Multiplier. Total procedural blanks for Re and Os are 2.7 ± 1.1
209 pg and 0.4 ± 0.4 pg, respectively, with an average $^{187}\text{Os}/^{188}\text{Os}$ of 0.37 ± 0.17 ($n = 2$, 1 SD).
210 The Re and Os uncertainties presented in Table 1 are determined by the full propagation of
211 uncertainties from the mass spectrometer measurements, blank abundances and isotopic
212 compositions, spike calibrations, and the results from analyses of Re and Os standards. The
213 Re standard data together with the accepted $^{185}\text{Re}/^{187}\text{Re}$ ratio (0.59738; Gramlich et al.,
214 1973) are used to correct for mass fractionation. The Re and Os standard solution
215 measurements performed during the two mass spectrometry runs were 0.5982 ± 0.0012
216 (Re std, $n = 2$) and 0.1608 ± 0.0002 (DROsS, $n = 2$), respectively, which agree with the
217 values reported by Finlay et al. (2011) and references therein.

3.3. Sulphur Isotope Analytical Protocol

220 Aliquants of pyrite samples for sulphur isotope analysis were taken from the quartz veins at
221 the same five locations as those used for the Re-Os geochronology (Table 1). Approximately
222 0.01g was used for the analysis, with the sulphur extracted as SO_2 from the pyrite by fusing
223 the sample under vacuum at 1076°C in a Cu_2O (200mg) matrix (Wilkinson & Wyre, 2005).
224 The sample was then analysed on a VG SIRA II mass spectrometer to obtain values for
225 $\delta^{66}\text{SO}_2$ which were converted to $\delta^{34}\text{S}$. Standard correction factors were applied (Craig,
226 1957). Results are given in conventional $\delta^{34}\text{S}$ notation relative to the Vienna Canon Diablo

227 troilite standard (V-CDT). The reproducibility based on full replicate analyses of internal
228 laboratory standards was ± 0.2 per mil (1σ).

229

230 **4. Field relationships of the quartz-pyrite veins**

231 The occurrence of quartz veins is a widely recognised, but little described phenomenon in
232 the rocks of the Assynt Terrane (e.g., the presence of quartz veins is noted in Sheraton et
233 al., 1973). Some generally foliation-parallel veins are clearly relatively late features that are
234 closely associated with shearing along Laxfordian shear zones and the development of
235 schistose, phyllosilicate-rich high strain zones (e.g., Beach, 1976; Beacom, 1999). However,
236 the present study has revealed that an earlier, much more widespread and distinctive group
237 of quartz-pyrite veins are present throughout the Assynt Terrane and at least part of the
238 Gruinard Terrane. The distribution of the quartz veins does not seem uniform – they typically
239 occur in clusters cutting the gneisses in regions covering areas of tens to hundreds of
240 square metres, with particularly well-defined groups recognised in the Loch Assynt and
241 Clashnessie regions of the Assynt Terrane, and along the trace of the CSZ (Fig. 1).

242 The quartz veins typically range in thickness from a few millimetres to several tens of
243 centimetres (e.g., Fig. 2a-e, g), and are relatively straight and continuous features that can
244 be traced for several metres or, less commonly, tens of metres along strike. They have
245 sharply-defined margins, are occasionally anastomosing and sometimes contain inclusions
246 of country-rock or clusters of pink K-feldspar. Pyrite is not found in all of the veins, but where
247 it occurs it is typically either located along the margins as large crystals (>0.5 mm) or as
248 large clusters (>1 cm) of crystals distributed sparsely throughout the veins (e.g., Fig. 2h). In
249 some cases pyrite clusters have been partially to completely oxidised to hematite or limonite,
250 particularly where they have been exposed at the surface for an extended period; this often
251 gives weathered veins a distinctive localised orange-red staining. Within the CSZ, pyrite
252 crystals are also sometimes found in the sheared gneisses surrounding the vein. In isolated
253 road cut exposures, the development of quartz-pyrite veins is additionally associated with a

254 localised yellow-brown sulphurous weathering of the gneisses, e.g., in roadcuts east of
 1
 2 255 Lochinver (National grid reference NC 1012 2366; Samples BH2 and 5; Table 1).

3
 4 256

5
 6 257 *4.1. Cross-cutting relationships*

7
 8 258 The quartz-pyrite veins display a consistent set of cross-cutting relationships with other
 9
 10 259 features in the Lewisian Complex. They typically cross-cut the oldest, moderately to
 11
 12 260 shallowly-dipping Badcallian foliations and folds (e.g., Fig. 2a), although in areas where the
 13
 14 261 foliation is particularly intense and of variable orientation (e.g. Clashnessie), the veins may
 15
 16 262 locally be concordant with the local foliation. The veins also consistently cross-cut the
 17
 18 263 steeply-dipping Inverian shear fabrics of the CSZ (e.g., Fig. 2b) and other minor shear zones
 19
 20 264 of this age within the terrane, as well as all observed Scourie dykes (e.g., Fig. 2c). Both
 21
 22 265 veins and dykes are consistently overprinted and reworked by dextral shear fabrics related
 23
 24 266 to the Laxfordian event, including the development of the central part of the CSZ (Attfield
 25
 26 267 1987; e.g., Fig. 2d). The quartz veins are also post-dated by 'late Laxfordian', epidote-
 27
 28 268 bearing small-scale shear zones and fractures, which exhibit a predominantly sinistral sense
 29
 30 269 of shear (e.g., Fig. 2e, f; see Beacom et al 2001). Many of the larger quartz vein clasts found
 31
 32 270 in the immediately overlying basal units of the Torridonian sandstones are plausibly derived
 33
 34 271 from the basement veins. The quartz-pyrite veins are everywhere cross-cut by gouge-
 35
 36 272 bearing Phanerozoic (post-Cambrian) normal faults (e.g., NC 1020 2360).

37
 38 273 Thus the field observations suggest that the quartz-pyrite veins post-date Badcallian
 39
 40 274 structures, the NW-SE trending Inverian fabrics and Scourie dykes. They appear to pre-date
 41
 42 275 all Laxfordian fabrics, 'late Laxfordian' faults, the deposition of the Torridonian sediments
 43
 44 276 and all post-Torridonian deformation episodes (mainly faulting).

45
 46 277

47
 48 278 *4.2. Orientation and kinematics*

49
 50 279 The orientations of 140 quartz-pyrite veins measured in the Assynt Terrane during the
 51
 52 280 present study are shown in Figures 3a-c, and the sparse lineations found on the veins in
 53
 54 281 Figure 3aii. A rose diagram plot (Fig. 3ai) suggests a predominance of NE-SW strikes with

55
 56
 57
 58
 59
 60
 61
 62
 63
 64
 65

282 subordinate NW-SE trends. The regional stereograms (Figs. 3biv-vi & c) better illustrate the
1 283 rather wider range of vein orientations, with a reasonably strong concentration of planes
2 3 striking NE-SW and, to a lesser extent NW-SE. Both sets display bimodal dip directions
4 284 (e.g., NW or SE and NE or SW, respectively; Figs. 3biv-vi & c). These observations suggest
5 6 285 a generally multimodal pattern of fracture orientations.
7 8 286

10 287 In order to investigate the possible effects on vein orientation of local country rock
11 288 fabrics and Laxfordian overprinting, the data have been plotted according to the age of the
12 13 289 local fabrics they cross-cut or are reworked by (Fig. 3b). In the regions of gneiss dominated
14 15 290 by the Badcallian event, both the foliations (Fig. 3bi) and the veins (Fig. 3biv) have large
16 17 291 variations in their orientations. The foliation shows a poorly-defined N-S trend dipping
18 19 292 shallowly W, whereas the veins show a reasonably strong NE-SW trend, with bimodal dips
20 21 293 steeply to the NW and rather more shallowly to the SE. The Inverian foliation has a strong
22 23 294 NW-SE trend with generally steep dips (Fig. 3bii), whereas the veins show a strong NE-SW
24 25 295 trend with dips mainly being steep and to the NW (Fig. 3bv). Both the Laxfordian foliation
26 27 296 and the veins within the Laxfordian fabrics show a strong NW-SE trend and steep dips (Figs.
28 29 30 31 297 3biii and vi), reflecting the strong reworking and reorientation of veins into parallelism with
32 33 298 those fabrics during overprinting deformation.
34 35 36 37

38 299 The data have also been plotted according to the localities where well-defined
39 40 300 clusters of veins are found (Figs. 3ci-vi). The stereoplots for localities such as Clashnessie
41 42 301 and Achmelvich areas (Figs. 3ci-ii) show a wide range of orientations whilst the best defined,
43 44 302 statistically significant trend is found in the Loch Assynt cluster (Fig. 3cv). Here there is a
45 46 303 very well-defined trend striking NE-SW with the majority of veins dipping steeply NW. It may
47 48 304 be significant that the pre-vein Badcallian foliation in this area is much weaker compared to
49 50 305 areas such as Clashnessie.
51 52

53 306 The kinematics of the quartz veins are difficult to deduce with any precision. Most of
54 55 307 the veins appear to be dilational (Mode 1 tensile) features based on observed offsets of
56 57 308 markers in the adjacent wall rocks, i.e., the vein opening directions lie at high angles to the
58 59 309 vein walls). A few large veins in the Loch Assynt and Lochinver regions display regular en
60 61 62 63 64 65

310 echelon off-shoots (e.g., Fig. 2g) consistent with some degree of vein-parallel shearing
 311 during emplacement (e.g. Peacock & Sanderson 1995). Of the seven veins found with such
 312 off-shoots, five indicated a sinistral and two a dextral sense of shear. There does not appear
 313 to be any obvious orientation control on the shearing directions, suggesting the shearing
 314 may be due to local strain heterogeneities. A few veins (n = 7) unaffected by Laxfordian
 315 reworking display poorly developed mainly oblique mineral lineations on their outer contacts
 316 (Fig. 3a_{ii}).

317

318 5. Rhenium-Osmium Geochronology

319 The total Re and Os abundances of the pyrite samples range from 6.8 to 25.8 ppb (parts per
 320 billion) and 298.8 to 660.5 ppt (parts per trillion; Table 1), respectively. The majority of the
 321 Os within the samples is radiogenic ^{187}Os (> 92 %). Four of the samples possess > 99 %
 322 radiogenic ^{187}Os (Table 1). As a result, the $^{187}\text{Re}/^{188}\text{Os}$ values are high to very high (265.6 to
 323 17531), with the accompanying $^{187}\text{Os}/^{188}\text{Os}$ values being very radiogenic (11.04 to 675.2).
 324 The predominance of radiogenic ^{187}Os ($^{187}\text{Os}'$) in the pyrite samples defines them as Low
 325 Level Highly Radiogenic (LLHR; Stein et al., 2000; Morelli et al., 2005). To account for the
 326 high-correlated uncertainties between the $^{187}\text{Re}/^{188}\text{Os}$ and $^{187}\text{Os}/^{188}\text{Os}$ data we present the
 327 latter with the associated uncertainty correlation value, *rho* (Ludwig, 1980), and the 2σ
 328 calculated uncertainties for $^{187}\text{Re}/^{188}\text{Os}$ and $^{187}\text{Os}/^{188}\text{Os}$ (Table 1). The regression of all the
 329 Re-Os data using *Isoplot V. 3.0* (Ludwig, 2003) and the ^{187}Re decay constant (λ) of
 330 $1.666 \times 10^{-11} \text{a}^{-1}$ (Smoliar et al., 1996) yields a Model 3 Re-Os age of 2259 ± 61 (2.9 %) Ma,
 331 with an initial $^{187}\text{Os}/^{188}\text{Os}$ of 0.9 ± 9.0 (2σ , Mean Squared Weighted Deviates [MSWD] = 22;
 332 Fig. 5a). Although the calculated Re-Os age has only a 2.9 % uncertainty, the high MSWD
 333 value (22) suggests that the degree of scatter about the regression line is a function of pyrite
 334 Re-Os systematics (discussed below). The imprecision of the initial $^{187}\text{Os}/^{188}\text{Os}$ does not
 335 permit an accurate evaluation of the origin of the Os in the pyrite, however the initial
 336 $^{187}\text{Os}/^{188}\text{Os}$ value, including the uncertainty, can be used to calculate the abundance of

337 $^{187}\text{Os}^r$ from the total ^{187}Os (common plus radiogenic) in the pyrite samples ($^{187}\text{Os}^{r1}$; Table 1).

338 The $^{187}\text{Os}^r$ is a product of ^{187}Re decay and model Re-Os dates for each sample can be

339 directly calculated using $t = \ln (^{187}\text{Os}^r / ^{187}\text{Re} = 1) / \lambda$. The model Re-Os dates, with the

340 exception of sample 64.1, all agree - within uncertainty - with the traditional $^{187}\text{Re}/^{188}\text{Os}$ vs

341 $^{187}\text{Os}/^{188}\text{Os}$ isochron age (Table 1; Fig. 5a). One sample from a vein cutting Badcallian

342 gneisses east of Lochinver (64.1; NC 1038, 2249) yields an imprecise model age of $1597 \pm$

343 1371.2 Ma. Although this date is within uncertainty of the other model ages and the Re-Os

344 isochron age, its nominal age is significantly younger (~ 800 Ma) than for the other five pyrite

345 samples. As such, sample 64.1 may represent a separate, distinct quartz and pyrite

346 mineralization event. If we consider this to be the case and regress the $^{187}\text{Re}/^{188}\text{Os}$ vs

347 $^{187}\text{Os}/^{188}\text{Os}$ data without sample 64.1, a $^{187}\text{Re}/^{188}\text{Os}$ vs $^{187}\text{Os}/^{188}\text{Os}$ age of 2249 ± 77 Ma, with

348 an initial $^{187}\text{Os}/^{188}\text{Os}$ of 3 ± 13 , is produced (2σ , MSWD = 15; Fig. 5a). This Re-Os isochron

349 age is within uncertainty of that determined from all the Re-Os data, but the degree of scatter

350 about the isochron is reduced (MSWD of 15 vs 22).

351 Isochron ages can also be determined by the regression of ^{187}Re vs $^{187}\text{Os}^r$ plus their

352 uncertainties. Excluding sample 64.1 for the reasons noted above, the ^{187}Re data together

353 with the $^{187}\text{Os}^r$ values ($^{187}\text{Os}^{r2}$; Table 2) calculated using the initial $^{187}\text{Os}/^{188}\text{Os}$ value (3 ± 13)

354 determined from the $^{187}\text{Re}/^{188}\text{Os}$ vs $^{187}\text{Os}/^{188}\text{Os}$ isochron without sample 64.1 (Fig. 5), a

355 ^{187}Re vs $^{187}\text{Os}^r$ isochron date of 2170 ± 180 Ma is obtained (Fig. 5b, initial $^{187}\text{Os} = 15 \pm 31$

356 ppt, MSWD = 0.6). We note that with the exception of sample 28 (Lochan Sgeireach) Re-Os

357 model ages calculated using $^{187}\text{Os}^r$ based on the initial $^{187}\text{Os}/^{188}\text{Os}$ value of 3 ± 13 are

358 extremely similar (Table 1). However, sample 28 yields a Model age ~ 450 Ma younger than

359 an age calculated using the initial of 0.9. Both calculated Model ages have very large

360 uncertainties. This sample possesses the least amount of $^{187}\text{Os}^r$ (~ 92 ppt – 73%), with its

361 abundance dramatically affected by the initial $^{187}\text{Os}/^{188}\text{Os}$ value (0.9 vs 3; Table 1).

362 A weighted average of the model Re-Os ages (not including sample 64.1; calculated

363 using a $^{187}\text{Os}^r$ based on the initial $^{187}\text{Os}/^{188}\text{Os}$ value of 3 ± 13) is 2248 ± 38 (MSWD = 0.6;

364 Fig. 5c). In summary, the ages determined from both the Re-Os isochron methods and the
1
2 365 weighted average of the Re-Os model ages are all within uncertainty. We favour using the
3
4 366 $^{187}\text{Re}/^{188}\text{Os}$ vs $^{187}\text{Os}/^{188}\text{Os}$ isochron age (without sample 64-1). From this study we consider
5
6 367 the majority of the pyrite mineralization and by inference the precipitation the quartz pyrite
7
8 368 veins and fracture formation occurred at 2249 ± 77 Ma.

10 369

13 370 **6. Sulphur Isotope Analysis**

15 371 All the samples from the sulphur isotope analysis yielded high amounts of sulphur (82 to,
16
17 372 97% yield). The $\delta^{34}\text{S}$ from the sulphides ranges from +3.0 to -2.2 per mil. All the samples
18
19 373 are slightly enriched in ^{34}S relative to 0 per mil, with the exception of sample 64.1, which has
20
21 374 a slightly depleted value of -2.2. This may suggest a slightly different source of the sulphur
22
23 375 for sample 64.1, and coupled with the Re-Os data may support a distinct quartz and pyrite
24
25 376 mineralization event from the other five samples. The range in the $\delta^{34}\text{S}$ values (+3.0 and -
26
27 377 2.2) encompasses that of the primitive mantle (Rollinson, 1993). The results therefore
28
29 378 suggest that the sulphur in the pyrite is most likely derived from a source not isotopically
30
31 379 fractionated from the primitive mantle value.

32 380

35 381 **7. Microstructural textures and inferred deformation mechanisms**

38 382 *7.1. Microstructural textures within quartz-pyrite veins*

40 383 The quartz-pyrite veins display an array of deformation textures suggesting that they have
41
42 384 experienced a complex history of deformation at different temperatures and pressures. A
43
44 385 number of overprinting relationships are seen which can be related to the relative chronology
45
46 386 of events seen in the field. The deformation textures are described below with reference to
47
48 387 the age of the country rock fabric which the veins either cross-cut or are overprinted by.

49 388

52 389 **7.1.1 Veins crosscutting Badcallian structures**

53
54
55
56
57
58
59
60
61
62
63
64
65

390 Despite modest amounts of grain-scale deformation, the veins cross-cutting Badcallian
1
2 391 gneisses (e.g., Fig. 2a, e) preserve a diverse range of deformation microstructures. The
3
4 392 most deformed examples contain large quartz crystals (> 1mm, but typically 3 – 7mm) that
5
6 393 show sweeping undulose extinction and have highly lobate grain boundaries as a result of
7
8 394 grain boundary migration processes during recrystallisation (Stipp et al., 2002). Chessboard
9
10 395 subgrains (e.g. Fig. 4a) within quartz crystals are also common and form in response to the
11
12 396 migration of dislocations within the crystal lattice into subgrain walls during recrystallisation
13
14 397 (e.g. Passchier and Trouw, 2005).

17 398 The least plastically deformed veins cutting Badcallian foliation are found on the
18
19 399 shores of Loch Assynt (e.g., Figs. 2e, g). The quartz crystals within these veins display
20
21 400 undulose extinction, whilst some larger grains contain deformation lamellae, which are zones
22
23 401 of differently orientated crystal lattice separated by dislocations. Grain boundaries have
24
25 402 undergone small-scale bulging during recrystallisation and small grains (<100µm) have
26
27 403 developed within the bulges and along the deformation lamellae (e.g., Fig. 4b).

30 404 Overall, the range of deformation microstructures observed in the quartz veins cutting
31
32 405 Badcallian gneisses suggests that they experienced small amounts of crystal plastic
33
34 406 deformation under moderate temperature (400 - 500°C) conditions. The veins on the shore
35
36 407 of Loch Assynt locally preserve rather lower temperatures textures (perhaps as low as
37
38 408 300°C) and/or higher strain rate conditions. This may be the result of 'late Laxfordian'
39
40 409 deformation associated with slip on the Loch Assynt Fault (e.g., like the structures shown in
41
42 410 Figs. 2e, f), to which they are proximal.

43
44
45
46 411

47 412 7.1.2 Veins cross-cutting Inverian structures

48
49 413 Veins emplaced into Lewisian gneisses reworked by Inverian deformation (e.g., Fig. 2b) also
50
51 414 show little obvious deformation at outcrop scale. A range of deformation microstructures are
52
53 415 preserved, including undulose extinction, deformation lamellae, new grain growth along
54
55 416 crystal boundaries, subgrain development and the development of lobate grain boundaries.
56
57 417 These are indicative of recrystallisation under low to moderate temperatures (350 - 500°C)
58
59
60
61
62
63
64
65

1 418 and high to moderate strain rates. Some veins contain large (>2mm) quartz crystals with
2 419 lobate boundaries, formed by grain boundary migration under moderate temperatures and
3
4 420 strain rates, which show grain boundary bulging and the development of new, small grains
5
6 421 (<250µm) within the bulges, particularly at triple-point grain boundaries (Fig. 4c). These
7
8 422 structures are typical of recrystallisation under somewhat lower temperatures (300 - 400°C),
9
10 423 and may indicate a lower temperature event. There is little evidence for this event within the
11
12 424 veins emplaced into Badcallian gneisses, and it may be that it is related to localised later
13
14 425 deformation and/or fluid flow restricted to the Inverian shear zones immediately following
15
16 426 vein emplacement. Alternatively, it may be a weak manifestation of Laxfordian deformation
17
18 427 given the regionally observed coincidence of Inverian and Laxfordian reworking (e.g. Attfield
19
20 428 1987).
21
22
23

24 429

26 430 7.1.3 Veins overprinted by Laxfordian structures

28 431 The veins emplaced within the Laxfordian part of the CSZ (e.g., Fig. 2d) have been heavily
29
30 432 reworked at outcrop scale. Many of the grain-scale textures resulting from the
31
32 433 recrystallisation of quartz are similar to those seen in the veins which were emplaced into
33
34 434 gneisses with Badcallian and Inverian foliations, but the finite strains are much higher. In
35
36 435 most veins, larger quartz crystals (>2mm) show sweeping undulose extinction, deformation
37
38 436 lamellae, subgrain development and lobate grain boundaries. These microstructures indicate
39
40 437 deformation under moderate temperatures (350 - 500°C) and strain rates. Relict S-C'
41
42 438 mylonite fabrics (e.g. Berthé et al. 1979; Snoke et al. 1998) are preserved in the most highly
43
44 439 deformed veins (e.g., Fig. 4d). Sub-parallel fine-grained (<100 µm) bands of feldspar,
45
46 440 muscovite and chlorite define the C-surfaces which are enclosed by polygonal quartz
47
48 441 aggregate (with grains sizes 0.5 – 3 mm). Quartz grain boundaries are often pinned by
49
50 442 aligned micas and some fine aligned grains are completely enclosed by much larger,
51
52 443 undeformed quartz grains (Fig. 4d). These fabrics are typical indicators of significant
53
54 444 secondary grain growth under elevated temperature conditions (e.g., Vernon 1976;
55
56 445 Passchier and Trouw, 2005).
57
58
59
60
61
62
63
64
65

446

1

2 447 7.1.4 Pyrite microstructural relationships

3

4 448 Pyrite occurs in a variety of forms in the veins of the Assynt Terrane. Some samples contain

5

6 449 large clusters of pyrite crystals up to 1.5cm in across (e.g., Fig. 2h) which are intimately

7

8 450 intergrown with quartz (e.g., Figs 4e, f). SEM images reveal the partial alteration of pyrite

9

10 451 grains to iron oxides along grain margins and fractures within some large pyrite clusters

11

12 452 (e.g., Fig. 4g, h). Small (<1mm) pyrite clusters are also associated with the mylonitized

13

14 453 quartz veins within the CSZ. There is little evidence for significant deformation of the pyrite

15

16 454 grains during recrystallization of the surrounding quartz aggregates even in cases where the

17

18 455 intensity of finite plastic strain is high.

19

20 456

21

22 457 7.1.5 Summary

23

24 458 The microstructural evidence from the veins suggests that most of the pyrite initially

25

26 459 crystallised at the same time as the quartz and that it is therefore a primary mineral phase.

27

28 460 The veins then experienced very modest amounts of deformation and recrystallisation during

29

30 461 a moderate temperature (350 - 500°C) and low strain rate strain rate event felt throughout

31

32 462 most of the Assynt Terrane. Given the similarity in quartz microstructures and interpreted

33

34 463 palaeotemperatures with the more highly deformed veins in the CSZ, it seems most likely

35

36 464 that the bulk of the modest deformations recorded here are also Laxfordian to 'late

37

38 465 Laxfordian' in age (ca. 1780-1400). Laxfordian deformation, especially within the CSZ,

39

40 466 resulted in the formation of mylonitic fabrics within the veins under mostly moderate

41

42 467 temperatures (350 - 500°C). There may also have been some limited remobilisation and re-

43

44 468 precipitation of pyrite related to fluid flow both within the veins and the adjacent sheared

45

46 469 gneisses.

47

48 470

49

50 471 **8. Discussion:**

51

52 472 The Re-Os isochron age obtained from the majority of the quartz-pyrite veins (2249 ± 77 Ma)

53

54 473 is consistent with our current understanding of the broad ages of regional

55

56

57

58

59

60

61

62

63

64

65

474 tectonometamorphic episodes in the Lewisian Complex (Fig. 6). Specifically, they cross cut
1
2 475 older Badcallian (*ca.* 2760 or 2480 Ma) and Inverian (*ca.* 2400-2480 Ma) fabrics and are
3
4 476 overprinted/reworked by younger Laxfordian (1790-1660 Ma) structures. The latter suggests
5
6 477 that the Re-Os systematics were not appreciably disturbed by structural reworking and the
7
8 478 upper greenschist conditions associated with the Laxfordian event.

11 479 The most recent U-Pb geochronology shows that intrusion of the Scourie dykes
12
13 480 predominantly occurred at 2391 – 2404 Ma, with moderately younger ages (2367 – 2372
14
15 481 Ma) at the SW edge of the Assynt Terrane (Davies and Heaman, 2014). The *ca.* 2250 Ma
16
17 482 age for the quartz-pyrite veins falls within the range of ages obtained from the NW-SE
18
19 483 trending Scourie dyke swarm across the entire Lewisian Complex (Fig. 6; 2418 Ma to 1991
20
21 484 Ma; Chapman 1979; Heaman and Tarney, 1989; Cohen et al., 1988; Waters et al., 1990;
22
23 485 Davies and Heaman, 2014). These studies suggest two main episodes of dyke intrusion at
24
25 486 *ca.* 2418 Ma and 1992 Ma (Fig. 6; Davies and Heaman, 2014), with distinct mantle sources
26
27 487 exploited during each event (Cartwright and Valley, 1991). The idea that there are multiple
28
29 488 episodes of ‘Scourie dyke’ intrusion is consistent with some geological field relationships. It
30
31 489 is known, for example, in the southern region of the Lewisian Complex that some ‘Scourie
32
33 490 dykes’ cut the Loch Maree Group metasediments and metavolcanics, which were thought to
34
35 491 have formed in oceanic basins and accreted to the continental crust through subduction
36
37 492 between 2000 and 1900 Ma (Park et al., 2001).

42 493 All the quartz-pyrite veins observed during the present study seen in the Assynt
43
44 494 Terrane cross-cut Scourie dykes, although this does not preclude the possibility that
45
46 495 regionally there may be some dykes that are younger. However, the Re-Os pyrite dating of
47
48 496 the veins at *ca.* 2250 Ma suggests a complex polyphase early Palaeoproterozoic tectonic
49
50 497 history of the Lewisian complex (Fig. 6). Veins form by the precipitation of minerals in dilating
51
52 498 hydrofractures and their regional development in clusters and swarms are indicative of
53
54 499 significant phase of fluid flow in the crust (e.g., Sibson, 1996 and references therein). The
55
56 500 simplest types of vein are Mode 1 fractures which open in the direction of the minimum
57
58 501 principle stress and have strike orientations perpendicular to it (e.g., Peacock & Mann,
59
60
61
62
63
64
65

502 2005). Most of the veins in the Assynt Terrane appear on the basis of their field relationships
1
2 503 to be Mode I features (e.g. Fig. 2a). If so, the prevalence of NE-SW strikes (e.g., Figs. 1, 3ai)
3
4 504 implies a NW-SE opening direction, although the veins show a wide range of other
5
6 505 orientations (Figs. 3b,c) which are attributed to a number of factors: the presence of highly
7
8 506 variable foliation in strongly banded gneisses; the presence of pre-existing fractures, or to
9
10
11 507 the reworking of veins by Laxfordian fabrics.

12
13 508 The pre-Laxfordian NE-SW orientation and inferred NW-SE opening directions of the
14
15 509 quartz-pyrite veins lie almost orthogonal to the regional NW-SE orientation – and inferred
16
17 510 NE-SW extension direction - of the Scourie dykes. If there are multiple episodes of Scourie
18
19 511 dykes on a regional scale, with some pre-dating and some post-dating the quartz-pyrite
20
21 512 veins, this implies that there were significant changes in the orientation of regional stress
22
23 513 vectors in the 500 Ma period between 2400 and 1900 Ma (Fig. 6). Note, however, that in
24
25 514 common with the Scourie dykes, the sulphur isotopic analysis of the quartz-pyrite veins is
26
27 515 suggestive of a source not isotopically fractionated from the primitive mantle derivation value
28
29 516 (Rollinson, 1993).

30
31
32
33 517 Although the Re-Os data for sample 64.1 provide a highly imprecise model age
34
35 518 (1597 ± 1356 Ma) its nominal age is considerably younger than the model ages for the other
36
37 519 samples ($2198.5 - 2328.7$ Ma), and, in addition, has the lowest Os abundance of ($242.8 \pm$
38
39 520 33.9 ppb) of all the samples. Furthermore, sample 64.1 is also the only sample with a
40
41 521 depleted $\delta^{34}\text{S}$ value (-2.2). Although this value could indicate that the sulphur source is not
42
43 522 isotopically fractionated from the primitive mantle value, like the other samples, it may be that
44
45 523 the sulphur within the pyrite has a slightly different origin to that found within other veins, or
46
47 524 that it may have been disturbed following emplacement, perhaps related to a later phase of
48
49 525 'late Laxfordian' brittle fracture fractures and fluid ingress. Further work and dating is
50
51 526 required to verify the age obtained and better constrain the geological and geochronological
52
53 527 significance of this younger age.

54
55
56
57
58 528
59
60 529 *8.1. Implications for terrane models*

1 530 Dating of the TTG protoliths suggests that the gneisses of the Gruinard Terrane are at least
2 531 100 Ma younger than those of the Assynt Terrane and underwent granulite metamorphism at
3
4 532 2730 Ma (Love et al., 2004; Park, 2005). Thus they are thought to belong to different and
5
6 533 separate Archaean terrane which amalgamated along the Strathan Line, south of Lochinver,
7
8 534 during Inverian folding and retrogression (Fig. 1, Love et al., 2004). The presence of post-
9
10
11 535 Inverian quartz-pyrite veins within both the Assynt and Gruinard Terranes is consistent with
12
13 536 this proposal.

14
15 537 The amphibolite-facies gneisses of the Rhiconich Terrane to the north have yielded
16
17 538 protolith ages of 2840-2800 Ma and a record magmatism at 2680 Ma (Kinny and Friend,
18
19 539 1997), but there is no apparent evidence of metamorphism at ca. 2780 Ma. This led Friend
20
21 540 and Kinny (2001) to suggest that the Assynt and Rhiconich Terranes were separate
22
23 541 Archaean crustal blocks of differing age and early history that were only finally juxtaposed by
24
25 542 a major episode of shearing during the along the Laxfordian Shear Zone at ca. 1750 Ma
26
27 543 (Fig. 1). This seems consistent with the apparent absence of ca. 2250 Ma quartz-pyrite veins
28
29 544 in the Rhiconich Terrane. However, recent fieldwork and dating by Goodenough et al. (2010;
30
31 545 2013) has found evidence that the Laxford Shear Zone initially formed as an Inverian
32
33 546 structure, pre-dating the intrusion of a regional suite of arc-related granitic sheets ca. 1880
34
35 547 Ma into both the Assynt and Rhiconich Terranes. These granites are then overprinted by the
36
37 548 main Laxfordian deformation and associated amphibolite-facies metamorphism, which
38
39 549 ranges from 1790-1670 Ma (Corfu et al., 1994; Kinny and Friend, 1997; Love et al., 2010). In
40
41 550 this case the absence of the quartz-pyrite veins to the north of the Laxford Shear Zone is
42
43 551 perhaps consistent with significant Laxfordian-age reactivation leading to final juxtaposition
44
45 552 of the two terranes.
46
47
48
49
50

51 553

52 554 **9. Conclusions**

53
54
55 555 A hitherto unrecognised set of quartz-pyrite veins have been identified in the Assynt and
56
57 556 Gruinard terranes of the Lewisian complex. The veins consistently cross-cut Badcallian and
58
59 557 Inverian structures in the gneisses, as well as (at least) the majority of Scourie dykes. They
60
61
62
63
64
65

558 are reworked during Laxfordian shearing events and are also cross cut by a range of later
 1
 2 559 brittle faulting events. The dominant strike direction of the quartz-pyrite veins suggests
 3
 4 560 emplacement during a regional NW-SE extension of the crust, whilst sulphur isotope
 5
 6 561 analyses of the pyrites are consistent with a primitive mantle origin for the fluids.

8
 9 562 The Re-Os date of 2249 ± 77 Ma for the pyrite within the veins is consistent with the
 10
 11 563 field relationships and other known geochronological constraints in the Lewisian Complex.
 12
 13 564 Both the Scourie dykes and quartz-pyrite veins are most likely developed as Mode I tensile
 14
 15 565 fractures, but their almost orthogonal present day orientations suggests that whilst the dykes
 16
 17 566 were emplaced during two or more periods of NE-SW crustal extension and associated
 18
 19 567 mafic magmatism ca. 1900-2400 Ma, the quartz-pyrite mineralization ca. 2250 Ma occurred
 20
 21 568 during an intervening phase of NW-SE extension.

23
 24 569 The presence of the quartz-pyrite veins in both the Assynt and Gruinard terranes
 25
 26 570 confirms their amalgamation prior to ca. 2250 Ma, most likely during the Inverian. The
 27
 28 571 apparent absence of the veins in the Rhiconich Terrane suggests it may not have been
 29
 30 572 finally amalgamated with the Assynt and Gruinard terranes until the Laxfordian. More
 31
 32 573 generally, this study demonstrates the potential value of the Re-Os technique as a means of
 33
 34 574 dating sulphide mineralisation events in continental basement terrains worldwide.

35
 36
 37
 38 575

40 576 **Acknowledgements**

41 577
 42 578 This research was supported, in part, by a student grant from the Geological Society of
 43
 44 579 London to RV. Rob Strachan, an anonymous reviewer and Randy Parrish are thanked for
 45
 46 580 their constructive comments and suggestions as reviewers.

47
 48
 49 581

51 582 **References**

52
 53 583 Attfield, P., 1987. The structural history of the Canisp Shear Zone, *In: Park, R.G. & Tarney,*
 54 584 *J. (eds), The early Precambrian rocks of Scotland and related rocks of Greenland,*
 55 585 *Department of Geology, Keele, 165-174.*
 56 586
 57 587 Beach, A., 1976. The interrelations of fluid transport, deformation, geochemistry and heat
 58 588 flow in early Proterozoic shear zones in the Lewisian complex, *Philosophical Transactions*
 59 589 *Royal Society London A, 280, 569-604.*

60
 61
 62
 63
 64
 65

590

- 1 591 Beacom, L.E., 1999. *The Kinematic Evolution of Reactivated and Non-Reactivated Faults in*
2 592 *Basement Rocks, NW Scotland*, Unpublished PhD thesis, Queens University, Belfast.
- 3 593
- 4 594 Beacom, L.E., Holdsworth, R.E., McCaffrey, K.J.W. & Anderson, T.B., 2001. A quantitative
5 595 study of the influence of pre-existing compositional and fabric heterogeneities upon fracture-
6 596 zone development during basement reaction, *In: Holdsworth, R.E., Strachan, R.A.,*
7 597 *Magloughlin, J.F. & Knipe, R.J, (eds). The Nature and Tectonic Significance of Fault Zone*
8 598 *Weakening*, Geological Society Special Publications, London, **186**, 195-211.
- 9 599
- 10 600 Berthé, D., Choukroune, P., and Jegouzo, P., 1979. Orthogneiss, mylonite and non coaxial
11 601 deformation of granites: the example of the South Armorican shear zone. *Journal of*
12 602 *Structural Geology*, 1, 31-43
- 13 603
- 14 604 Cameron, E.M., 1994. Depletion of gold and LILE in the lower crust: Lewisian Complex,
15 605 Scotland, *Journal of the Geological Society*, **151**, 747-754.
- 16 606
- 17 607 Cartwright, I. & Valley, J.W. 1991. Low-¹⁸O Scourie dike magmas from the Lewisian
18 608 complex, northwestern Scotland. *Geology* 19, 578-581.
- 19 609
- 20 610 Chapman, H.J. 1979. 2,390 Myr Rb-Sr whole-rock age for the Scourie dykes of north-west
21 611 Scotland. *Nature*, 277, 642-3.
- 22 612
- 23 613 Chattopadhyay, A., Holdsworth, R.E., McCaffrey, K.J.W. & Wilson, R.W. 2010. Recording
24 614 and Analyzing Geospatially Accurate Structural Data through 'Digital Mapping' Technique: A
25 615 Case Study from the Canisp Shear Zone, NW Scotland. *Journal of the Geological Society of*
26 616 *India*, **75**, 43-59.
- 27 617
- 28 618 Cohen, A.S., Waters, F.G., O'Nions, R.K. & O'Hara, M.J., 1988. A precise crystallisation age
29 619 for the Scourie Dykes, and a new chronology for crustal development in north-west Scotland.
30 620 *Chemical Geology*, **70**, 19.
- 31 621
- 32 622 Coleman, M.L. & Moore, M.P., 1978. Direct Reduction of Sulfates to Sulfur Dioxide for
33 623 Isotopic Analysis, *Analytical Chemical Society*, **50**, 1594-1595.
- 34 624
- 35 625 Corfu, F., Heaman, L.M. & Rogers, G. 1994: Polymetamorphic evolution of the Lewisian
36 626 complex, NW Scotland, as recorded by U-Pb isotopic compositions of zircon, titanite and
37 627 rutile. *Contributions to Mineralogy and Petrology*, **117**, 215-228.
- 38 628
- 39 629 Coward, M.P. & Park, R.G., 1987. The role of mid-crustal shear zones in the Early
40 630 Proterozoic evolution of the Lewisian, In; Park, R.G. & Tarney, J. (eds), *Evolution of the*
41 631 *Lewisian and Comparable Precambrian High Grade Terrains*, Geological Society Special
42 632 Publications, London, **27**, 127-138.
- 43 633
- 44 634 Craig, H., 1957. Isotopic standards for carbon and oxygen and correction factors for mass-
45 635 spectrometric analysis of carbon dioxide, *Geochimica et Cosmochimica*, **12**, 133-149.
- 46 636
- 47 637 Davies, J.H.F.L. & Heaman, L.M., 2014, New U-Pb baddeleyite and zircon ages for the
48 638 Scourie dyke swarm: A long-lived large igneous province with implications for the
49 639 Paleoproterozoic evolution of NW Scotland. *Precambrian Research*, In Press..
- 50 640
- 51 641 Dickinson, B.B. & Watson, J., 1976. Variations in crustal level and geothermal gradient
52 642 during the evolution of the Lewisian Complex of Northwest Scotland, *Precambrian Research*,
53 643 **3**, 363-374.
- 54 644
- 55
- 56
- 57
- 58
- 59
- 60
- 61
- 62
- 63
- 64
- 65

- 645 Droop, G.T.R., Fernandes, L.A.D. & Shaw, S., 1989. Laxfordian metamorphic conditions of
1 646 the Palaeoproterozoic Loch Maree Group, Lewisian Complex, NW Scotland, *Scottish*
2 647 *Journal of Geology*, **35**, 31-50.
- 3 648
4 649 Finlay, A. J., Selby, D., Osborne, M., 2011. Re-Os geochronology and fingerprinting of
5 650 United Kingdom Atlantic Margin oil: Temporal Implications for regional petroleum systems,
6 651 *Geology*, **39**, 475-478.
- 7 652
8 653 Friend, C.R.L. & Kinny, P.D. 1995. New evidence for the protolith ages of Lewisian
9 654 granulites, northwest Scotland. *Geology*, **23**, 1027–1030.
- 10 655
11 656 Friend, C.R.L. & Kinny, P.D. 2001. A reappraisal of the Lewisian Gneiss Complex:
12 657 geochronological evidence for its tectonic assembly from disparate terranes in the
13 658 Proterozoic, *Contribution to Mineralogy and Petrology*, **142**, 198-218.
- 14 659
15 660 Goodenough, K.M., Park, R.G., Krabbendam, M., Myers, J.S., Wheeler, J., Loughlin, S.,
16 661 Crowley, Q., L.F.C.R., Beach, A., Kinny, P.D., Graham, R., 2010. The Laxford Shear Zone:
17 662 an end-Archaeon terrane boundary? In: Law, R., Butler, R.W.H., Holdsworth, R.E.,
18 663 Krabbendam, M., Strachan, R. (eds.), *Continental Tectonics and Mountain Building*.
19 664 Geological Society Special Publication, **335**, 103-120.
- 20 665
21 666 Goodenough, K.M., Crowley, Q.G., Krabbendam, M. & Parry, S.E. 2013. New U-Pb age
22 667 constraints for the Laxford Shear Zone, NW Scotland: Evidence for tectono-magmatic
23 668 processes associated with the formation of a Palaeoproterozoic supercontinent.
24 669 *Precambrian Research*, **233**, 1-19.
- 25 670
26 671 Gramlich, J.W., Murphy, T.J., Garner, E.L. & Shields, W.R., 1973. Absolute isotopic
27 672 abundance ratio and atomic weight of a reference sample of rhenium, *Journal of Research*
28 673 *of the National Bureau of Standards*, **77A**, 691–698.
- 29 674
30 675 Hamilton, P.J., Evensen, N.M., O’Nions, R.K., Tarney, J., 1979. Sm-Nd systematics of
31 676 Lewisian gneisses: implications for the origin of granulites. *Nature*, **277**, 25–28.
- 32 677
33 678 Heaman, L.M. & Tarney, J., 1989. U-Pb baddeleyite ages for the Scourie dyke swarm,
34 679 Scotland: evidence for two distinct intrusion events, *Nature*, **340**, 705-708.
- 35 680
36 681 Jensen, L.N., 1984. Quartz microfabric of the Laxfordian Canisp Shear Zone, NW Scotland,
37 682 *Journal of Structural Geology*, **6**, 293-302.
- 38 683
39 684 Kinny, P., Friend, C., 1997. U-Pb isotopic evidence for the accretion of different crustal
40 685 blocks to form the Lewisian Complex of Northwest Scotland. *Contributions to Mineralogy and*
41 686 *Petrology*, **129**, 326–340.
- 42 687
43 688 Kinny, P.D., Friend, C.R.L. & Love, G.L., 2005. Proposal for a terrane-based nomenclature
44 689 for the Lewisian Gneiss Complex of NW Scotland, *Journal of the Geological Society*, **162**,
45 690 175-186.
- 46 691
47 692 Love, G.J.L, Kinny, P.D. & Friend, C.R.L., 2004. Timing of magmatism and metamorphism in
48 693 the Gruinard Bay area of the Lewisian Gneiss Complex: comparisons with the Assynt
49 694 Terrane and implications for terrane accretion, *Contributions to Mineralogy and Petrology*,
50 695 **146**, 620-636.
- 51 696
52 697 Love, G.J., Friend, C.R.L., Kinny, P.D., 2010. Palaeoproterozoic terrane assembly in the
53 698 Lewisian Gneiss Complex on the Scottish mainland, south of Gruinard Bay: SHRIMP U–Pb
54 699 zircon evidence. *Precambrian Research*, **183**, 89–111.
- 55
56
57
58
59
60
61
62
63
64
65

- 700
1 701 Ludwig, K.R., 1980, Calculation of uncertainties of U-Pb isotope data: *Earth and Planetary*
2 702 *Science Letters*, **46**, 212–220.
3 703
4 704 Ludwig, K.R., 2003, Isoplot/Ex, version 3: A geochronological toolkit for Microsoft Excel:
5 705 Berkeley, CA, Geochronology Center Berkeley.
6 706
7 707 Moorbath, S., Welke, H., Gale, N., 1969. The significance of lead isotope studies in ancient,
8 708 high-grade metamorphic basement complexes, as exemplified by the Lewisian rocks of
9 709 Northwest Scotland. *Earth and Planetary Science Letters*, **6**, 245–256.
10 710
11 711 Morelli, R.M., Creaser, R.A., Selby, D., Kontak, D.J. and Horne, R.J., 2005, Rhenium-
12 712 Osmium arsenopyrite geochronology of Meguma Group gold deposits, Meguma terrane,
13 713 Nova Scotia, Canada: Evidence for multiple gold mineralizing events, *Economic Geology*,
14 714 **100**, 1229–1242.
15 715
16 716 O’Hara, M.J. 1961. Petrology of the Scourie Dyke, Sutherland. *Mineralogical Magazine*, **32**,
17 717 848-865.
18 718
19 719 Park, R.G., 1970. Observations on Lewisian chronology. *Scottish Journal of Geology*, **6**,
20 720 379–399.
21 721
22 722 Park, R.G., 2005. The Lewisian terrane model: a review, *Scottish Journal of Geology*, **41**,
23 723 105-118.
24 724
25 725 Park., R.G. & Tarney, J., 1987. The Lewisian Complex: a typical Precambrian high-grade
26 726 terrane?, In: Park, R.G. & Tarney, J. (eds), *Evolution of the Lewisian and Comparable*
27 727 *Precambrian High Grade Terranes*, Geological Society, London, 13-26.
28 728
29 729 Park, R.G., Cliff, R.A., Fettes, D.J., Stewart A.D., 1994. Precambrian rocks in northwest
30 730 Scotland west of the Moine Thrust: the Lewisian Complex and the Totridonian. In: W.
31 731 Gibbons and A.L. Harris (Editors), *A Revised Correlation of Precambrian Rocks in the British*
32 732 *Isles*. Geological Society of London Special Report, **22**, 6-22.
33 733
34 734 Park, R.G, Tarney, J. & Connelly, J.N., 2001. The Loch Maree Group: Palaeoproterozoic
35 735 subduction-accretion complex in the Lewisian of NW Scotland, *Precambrian Research*, **105**,
36 736 205-226.
37 737
38 738 Park, R.G., Stewart, A.D. & Wright, D.T. 2002. The Hebridean Terrane. In: Trewin, N.H. (ed)
39 739 *The Geology of Scotland*. Geological Society, London, 45-80.
40 740
41 741 Passchier, C.W. & Trouw, R.A.J., 2005. *Micro-Tectonics*, Springer Berlin Heidelberg, New
42 742 York, 25-66.
43 743
44 744 Peacock, D.C.P. & Mann, A., 2005. Evaluation of the controls on fracturing in reservoir
45 745 rocks, *Journal of Petroleum Geology*, **28**, 385-396.
46 746
47 747 Peacock, D.C.P. & Sanderson, D.J. 1995. Pull-aparts, shear fractures and pressure solution.
48 748 *Tectonophysics*, 241, (1-2), 1-13.
49 749
50 750 Rollinson, H., 1993. *Using Geochemical Data: evaluation, presentation, interpretation*,
51 751 Longman Group UK Ltd, Harlow, 303-306.
52 752
53
54
55
56
57
58
59
60
61
62
63
64
65

- 753 Selby, D., Kelley, K.D., Hitzman, M.W. & Zieg, J., 2009. Re-Os sulphide (Bornite,
 1 754 Chalcopyrite, and Pyrite) systematic of the Carbonate-hosted copper deposits at Ruby
 2 755 Creek, Southern Brooks Range, Alaska, *Economic Geology*, **104**, 437-444.
 3 756
- 4 757 Sibson, R.H. 1996. Structural permeability of fluid-driven fault-fracture meshes. *Journal of*
 5 758 *Structural Geology*, **18**, 1031–1042.
 6 759
- 8 760 Sheraton, J.W., Tarney, J., Wheatley, T.J. & Wright, A.E., 1973. The structural history of the
 9 761 Assynt district, In: Park, R.G. & Tarney, J. (eds), *The early Precambrian rocks of Scotland*
 10 762 *and related rocks of Greenland*, Department of Geology, Keele, 13-30.
 11 763
- 12 764 Smoliar, M.I., Walker, R.J., & Morgan, J.W., 1996. Re-Os isotope constraints on the age of
 13 765 Group IIA, IIIA, IVA, and IVB iron meteorites, *Science*, **271**, 1099–1102.
 14 766
- 15 767 Snoke, A.W., Tullis, J. and Todd, V.R., 1998. *Fault-related Rocks*. Princeton University
 16 768 Press, Princeton New Jersey, New Jersey, 617 pp.
 17 769
- 19 770 Stein, H.J., Morgan, J.W. & Schersten, A., 2000. Re-Os of Low-Level Highly Radiogenic
 20 771 (LLHR) Sulphides: The Hurnas Gold Deposit, Southwest Sweden, Records Continental-Scle
 21 772 Tectonic Events, *Economic Geology*, **95**, 1657-1671.
 22 773
- 23 774 Stipp, M., Stunitz, H., Heilbronner, R. & Schmid, S.M., 2002. The eastern Tonale fault zone:
 24 775 a 'natural laboratory' for crystal plastic deformation of quartz over a temperature range from
 25 776 250 to 700°C, *Journal of Structural Geology*, **24**, 1861-1884.
 26 777
- 28 778 Sutton, J. & Watson, J., 1951. The pre-Torridonian metamorphic history of the Loch Torridon
 29 779 and Scourie areas in the north-west Highlands, and its bearing on the chronological
 30 780 classification of the Lewisian, *Quarterly Journal of the Geological Society*, **106**, 241-307.
 31 781
- 32 782 Tarney, J., 1973. The Scourie dyke suite and the nature of the Inverian event in Assynt, In:
 33 783 Park, R.G. & Tarney, J. (eds), *The early Precambrian rocks of Scotland and related rocks of*
 34 784 *Greenland*, Department of Geology, Keele, 31-44.
 35 785
- 36 786 Vernon, R.H. 1976. *Metamorphic Processes: Reactions and Microstructure Development*.
 37 787 George Allen & Unwin, pp 247.
 38 788
- 40 789 Waters, F.G., Cohen, A.S., O'Nions, R.K. & O'Hara, M.J., 1990. Development of Archaean
 41 790 lithosphere deduced from chronology and isotope chemistry of Scourie Dykes, *Earth and*
 42 791 *Planetary Science Letters*, **97**, 241-255.
 43 792
- 44 793 Wheeler, J., Park, R.G., Rollinson, H.R. & Beach, A., 2010. The Lewisian Complex: insights
 45 794 into deep crustal evolution, In: Law, R.D., Butler, R.W., Holdsworth, R.E., Krabbendam, M. &
 46 795 Strachan, R.A. (eds), *Continental Tectonics and Mountain Buildings: The Legacy of Peach*
 47 796 *and Horne*, Geological Society, London, Special Publications, **335**, 51-79.
 48 796
 49 797
- 50 798 Wilkinson, J.J. & Wyre, S.L., 2005. Ore-Forming Processes in Irish-Type Carbonate-hosted
 51 799 Zn-Pb Deposits: Evidence from Mineralogy, Chemistry, and Isotopic Composition of
 52 800 Sulphides at the Lisheen Mine. *Economic Geology*, **100**, 63-86.
 53 801
- 54 802 Zhu, X.K., O'Nions, R.K., Belshaw, N.S., Gibb, A.J., 1997. Lewisian crustal history from in
 55 803 situ SIMS mineral chronometry and related metamorphic textures. *Chemical Geology*, **136**,
 56 804 205–218.
 57 804
 58 805

60 806 Figure Captions

61
 62
 63
 64
 65

807 **Figure 1)** Highly simplified geological map showing the location and orientations of the
 808 quartz vein clusters (i-vi) studied within the Assynt Terrane of the Lewisian Complex. Note
 809 that this is not an exhaustive assessment of all quartz veins present in the Assynt Terrane,
 810 i.e. there may be many more clusters than are shown here. Inset map shows general
 811 location in Scotland and main Lewisian Complex terranes discussed in this paper.

812
 813 **Figure 2)** Field relationships of quartz-pyrite veins. a) NE-SW vein cross-cutting shallowly-
 814 NW-dipping Badcallian foliation near Clashnessie (NC 0855 3102). Note offset of layers
 815 across vein indicating Mode I tensile opening (arrows); b) NE-SW vein (below hammer)
 816 cross-cutting steep NW-SE Inverian foliation in Canisp Shear Zone (NC 0521 2593); c) NE-
 817 SW vein cross-cutting Scourie dyke on the shore of Loch Assynt (NC 2135 2510); d) NW-SE
 818 vein folded and reworked by Laxfordian fabrics, Canisp Shear Zone (NC 0515 2620); e) NE-
 819 SW vein cut and offset 10cm by NW-SE sinistral brittle fault in Badcallian gneisses close to
 820 the trace of the Loch Assynt Fault (NC 2110 2517); f) En echelon tensile fractures filled with
 821 epidote indicating sinistral shear in Badcallian gneisses close to the trace of the Loch Assynt
 822 Fault (NC 2110 2517); g) ENE-WSW vein with en-echelon off-shoots, indicating a small
 823 component of sinistral shear parallel to the vein margins (NC 2135 2510); h) Large pyrite
 824 cluster within a quartz vein (NC1038 2249). Note fracturing of pyrite and characteristic iron
 825 oxide staining.

826 **Figure 3)** Orientation data for the regional quartz-pyrite vein suite. a) i) Rose diagram of vein
 827 trends for the entire Assynt Terrane (for locality-based versions, see Fig. 1), ii) lower
 828 hemisphere equal-area stereoplots of veins with lineated margins; b) Equal area stereoplots
 829 of gneiss foliations (i-iii) and of associated veins from each locality (iv-vi) grouped according
 830 to the inferred age of the wall rock fabric; c) Equal area stereoplots of quartz vein clusters
 831 measured in the six localities (i-vi) shown in Fig 1.

832 **Figure 4)** Representative microstructures of quartz-pyrite veins viewed using optical
 833 microscope and FESEM. a) Chess-board extinction in large quartz crystals from vein cutting

834 Badcallian gneisses at Kylesku; b) New grains forming along grain boundaries and
 1 deformation lamellae, reflecting slightly lower temperature overprint in vein located close to
 2 835 the trace of the Loch Assynt Fault; c) Development of new grains at triple junction grain
 3
 4 836 boundaries overprinting higher temperature deformation features in vein cutting Inverian
 5
 6 837 fabrics near Lochinver; d) Recrystallised S-C fabric in highly sheared veing from the
 7
 8 838 Laxfordian central part of the Canisp Shear Zone, e) Quartz intergrown with within blocky
 9
 10 839 pyrite cluster; f) Intricate intergrowths of pyrite and quartz from vein cutting Scourie dyke at
 11
 12 840 Loch Assynt; g) BSEM image of smooth pyrite (light grey) intergrown with quartz (dark grey)
 13
 14 841 from the same sample as f). The radial fibrous material is iron oxide replacing pyrite; h)
 15
 16 842 Alteration of pyrite (bright grey) along fractures to iron oxides (darker mottled greys), Sample
 17
 18 843 64.1 (see text for details). Note that all the optical micrographs are cross-polar views.
 19
 20 844
 21
 22 845

26 846 **Figure 5)** Re-Os data for the pyrite from the quartz-pyrite veins. A) $^{187}\text{Re}/^{188}\text{Os}$ and
 27
 28 847 $^{187}\text{Os}/^{188}\text{Os}$ plot for all samples and all samples minus sample 64.1; B) ^{187}Re vs $^{187}\text{Os}^r$ plot,
 29
 30 848 with the $^{187}\text{Os}^r$ data calculated using an initial of 3 ± 13 ; C) Weighted average of Re-Os
 31
 32 849 model ages, with the model ages calculated using an initial of 3 ± 13 . See text for
 33
 34 850 discussion.
 35
 36 851

40 852 **Figure 6)** The chronology of events during the Archaean to Proterozoic in the Assynt
 41
 42 853 Terrane, showing the range of possible Scourie dyke episodes and the vein emplacement
 43
 44 854 period ascertained during the present study.
 45
 46 855

50 856 **Table Caption**

53 857 **Table 1)** Re-Os and S isotope data for pyrite from quartz veins in the Lewisian Complex, NW
 54
 55 858 Scotland. All uncertainities are reported at the 2s level, $^{187}\text{Os}/^{188}\text{Os}$ uncertainities reported at
 56
 57 859 2SE; all data are blank corrected, blanks for Re and Os were 2.7 ± 1.1 and 0.40 ± 0.42 pg,
 58
 59 860 respectively, with an average $^{187}\text{Os}/^{188}\text{Os}$ value of 0.37 ± 0.17 (1SD, n = 2). All uncertainities
 60
 61
 62
 63
 64
 65

861 are determined through the full propagation of uncertainties of the Re and Os mass
 1 spectrometer measurements, blank abundances and isotopic compositions, spike
 2 862 calibrations, and reproducibility of standard Re and Os isotopic values. $^{187}\text{Os}^r$ presented are
 3
 4 863 calculated using initial $^{187}\text{Os}/^{188}\text{Os}$, plus its uncertainty, from regression of data using
 5
 6 864 $^{187}\text{Re}/^{188}\text{Os}$ vs. $^{187}\text{Os}/^{188}\text{Os}$ isochron plot; rho is the error correlation.
 7
 8 865

10 866 1= $^{187}\text{Os}^r$ determined from an initial $^{187}\text{Os}/^{188}\text{Os}$ of 0.9 ± 9.0 (Fig. 5A).

12 867 2= $^{187}\text{Os}^r$ determined from an initial $^{187}\text{Os}/^{188}\text{Os}$ of 3 ± 13 (Fig. 5A). With the exception of
 13
 14 868 sample RO297-3/28, the calculated % $^{187}\text{Os}^r$ is very similar using either initial $^{187}\text{Os}/^{188}\text{Os}$
 15
 16 869 values of 0.9 ± 9.0 or 3 ± 13 . For sample RO297-3/28 the % $^{187}\text{Os}^r$ decreases to ~72.8%
 17
 18 870 using an initial $^{187}\text{Os}/^{188}\text{Os}$ value of 3 ± 13 . A model age can be directly calculated using

$$21 \quad 871 \quad ^{187}\text{Os}^r/^{187}\text{Re} = e^{t\lambda} - 1$$

22 872 3 = Model age determined using an initial $^{187}\text{Os}/^{188}\text{Os}$ value of 0.9 ± 9.0 (Fig. 5A).

23 873 4 = Model age determined using an initial $^{187}\text{Os}/^{188}\text{Os}$ value of 3 ± 13 (Fig. 5A).

24 874 5 = The reproducibility based on full replicate analyses of internal laboratory standards was
 25
 26
 27
 28
 29
 30
 31 875 ± 0.2 per mil (1σ).

32
 33 876
 34
 35
 36
 37
 38
 39
 40
 41
 42
 43
 44
 45
 46
 47
 48
 49
 50
 51
 52
 53
 54
 55
 56
 57
 58
 59
 60
 61
 62
 63
 64
 65

1
2
3 1
4 2 Structural characteristics and Re-Os dating of quartz-pyrite veins in the
5
6
7 3 Lewisian Gneiss Complex, NW Scotland: evidence of an Early
8
9 4 Paleoproterozoic hydrothermal regime during terrane amalgamation.
10
11 5

12
13 6 R. Vernon^{1*}, R.E. Holdsworth^{1†}, D. Selby¹, E. Dempsey¹, A. J. Finlay¹ & A.F. E. Fallick²
14
15 7

16
17 8 ¹ Department of Earth Sciences, Durham University, Durham, DH1 3LE, UK.

18
19 9 ² SUERC, Scottish Enterprise Technology Park, Rankine Avenue, East Kilbride, G75 0QF,
20
21 10 UK.

22 11 *Current address: Department of Geology, University of Leicester, University Road,
23
24 12 Leicester, LE1 7RH, UK.

25
26 13 †Corresponding author
27
28 14

29
30 15 **Abstract:** In the Archaean basement rocks of the Assynt and Gruinard terranes of the
31
32 16 mainland Lewisian Complex in NW Scotland, a regional suite of quartz-pyrite veins cross-cut
33
34 17 regional Palaeoproterozoic (Badcallian, [eaca.](#) 2700 Ma; Inverian, [eaca.](#) 2480 Ma) fabrics
35
36 18 and associated Scourie dykes. The quartz veins are overprinted by amphibolite-greenschist
37
38 19 facies Laxfordian deformation fabrics ([eaca.](#) 1760 Ma) and later brittle faults. The
39
40 20 hydrothermal mineral veins comprise a multimodal system of tensile/hybrid hydraulic
41
42 21 fractures which are inferred to have formed during a regional phase of NW-SE extension.
43
44 22 The almost orthogonal orientation of the quartz veins (NE-SW) to the Scourie dykes (NW-
45
46 23 SE) are incompatible and must result from distinct paleostress regimes suggesting they are
47
48 24 related to different tectonic events. This hypothesis is supported by Rhenium-Osmium dating
49
50 25 of pyrite that yields an age of 2249 ± 77 Ma, placing the vein-hosted mineralisation event
51
52 26 after the oldest published dates for the Scourie Dykes (2420 Ma), but before the youngest
53
54 27 ages (1990 Ma). Sulphur isotope analysis suggests that the sulphur associated with the
55
56
57
58
59
60
61
62
63
64
65

1
2
3 28 | pyrite is isotopically indistinguishable from~~ef~~ primitive mantle-~~origin~~. The presence of the
4
5 29 | eo~~ca~~. 2250 Ma quartz-pyrite veins in both the Assynt and Gruinard terranes confirms that
6
7 30 | these crustal units were amalgamated during or prior to Inverian deformation. The absence
8
9 31 | of the veins in the Rhiconich Terrane is consistent with the suggestion that it was not finally
10
11 32 | amalgamated to the Assynt Terrane until the Laxfordian.

12 33 | **[End]**
13
14
15
16
17
18
19
20
21
22
23
24
25
26
27
28
29
30
31
32
33
34
35
36
37
38
39
40
41
42
43
44
45
46
47
48
49
50
51
52
53
54
55
56
57
58
59
60
61
62
63
64
65

1. Introduction

The Archaean gneisses of the Lewisian Complex in NW Scotland form a well exposed and relatively accessible area of Laurentian continental basement rocks that lie in the immediate foreland region of the Palaeozoic Caledonian Orogen (Fig. 1). Like many regions of continental metamorphic basement, the Lewisian Complex preserves evidence for multiple episodes of igneous intrusion, ductile and brittle deformation together with associated phases of metamorphism and mineralisation (e.g. Sutton and Watson 1951; Park 1970; Beacom et al., 2001; Wheeler et al., 2010). Whilst cross-cutting and overprinting relationships observed in the field and thin section allow *relative* age relationships to be established on both regional and local scales, only radiometric ages are able to give information concerning the absolute timing of events. Despite the emergence of an increasing number of geochronometers for Earth Scientists, an enduring problem in many basement regions is a relative paucity of material suitable for reliable radiometric dating. This lack of absolute age determinations has become a particularly significant problem in the Lewisian Complex since Kinny et al. (2005) and Friend and Kinny (2001) proposed that the Lewisian may comprise a number of lithologically and geochronologically distinct tectonic units or terranes assembled progressively during a series of Precambrian amalgamation episodes perhaps spanning more than a billion years (see Park, 2005; Goodenough et al., 2013 for discussions).

This paper describes the lithology, field relationships and microstructures of a little described set of quartz-pyrite veins that are recognised throughout the Assynt Terrane and within the Gruinard Terrane. These mineralised hydrofractures display a consistent set of contact relationships relative to regionally recognised igneous, metamorphic and deformational events. Rhenium-osmium (Re-Os) geochronology on pyrites collected from these veins is used to obtain a consistent set of ages that better constrain the absolute timing of events in this important part of the Lewisian Complex in NW Scotland. It also illustrates the potential value of the Re-Os technique as a means of dating sulphide mineralisation events in geologically complex continental basement terrains worldwide.

1
2
3 62
4
5 63
6
7 64
8
9 65
10 66
11
12 67
13
14 68
15
16 69
17
18 70
19
20 71
21 72
22
23 73
24
25 74
26
27 75
28
29 76
30
31 77
32 78
33
34 79
35
36 80
37
38 81
39
40 82
41
42 83
43 84
44
45 85
46
47 86
48
49 87
50
51 88
52
53 89
54
55
56
57
58
59
60
61
62
63
64
65

2. Regional Setting

The Precambrian rocks of the Lewisian Complex of NW Scotland form a fragment of the continental basement of Laurentia that lies to the west of the Caledonian Moine Thrust (Fig. 1). The rocks are for the most part little affected by Caledonian deformation and have experienced a number of major crustal-scale geological events during the Archaean and Palaeoproterozoic. The Lewisian Complex is divided into a number of tectonic regions or terranes which are predominantly separated by steeply-dipping shear zones or faults (e.g. Park et al., 2002; Park, 2005).

The Assynt Terrane (Fig. 1) forms the central part of the Lewisian Complex in mainland NW Scotland. It comprises grey, banded, tonalite-trondjemite-granodioritic (TTG) gneisses which are locally highly heterogeneous lithologically, ranging from ultramafic to acidic compositions (e.g., Sheraton et al., 1973). The TTG gneisses are thought to be derived from igneous plutons intruded at 3030 to 2960 Ma (high precision U-Pb and Sm-Nd geochronology; Hamilton et al., 1979; Friend and Kinny, 1995; Kinny and Friend, 1997). These rocks then underwent deformation and granulite-facies metamorphism during the so-called Badcallian event(s) which led to significant depletion of large-ion lithophile elements in the TTG gneisses that is more extensive in the Assynt Terrane compared to adjacent amphibolite-facies terranes (e.g. Rhiconich, Gruinard; Moorbath et al., 1969; Cameron, 1994; Wheeler et al., 2010). The timing of Badcallian events are incompletely resolved with current age constraints suggesting either [eaca.](#) 2760 Ma (e.g., Corfu et al. 1994; Zhu et al., 1997), and/or [eaca.](#) 2490 - 2480 Ma (e.g., Friend and Kinny 1995; Kinny & Friend, 1997).

The central part of the Assynt Terrane is cut by the major NW-SE-trending, steeply dipping dextral transpressional Canisp Shear Zone (CSZ) which has a maximum width of 1.5km (Attfield, 1987; Fig. 12). There are also many other smaller steeply-dipping, NW-SE to WNW-ESE trending minor shear zones cutting the surrounding Badcallian gneisses (Park and Tarney, 1987). Some of these shear zones, including the CSZ, developed initially during Inverian deformation and amphibolites-facies retrogression which affected substantial parts

1
2
3 90 of the Assynt Terrane. The absolute age of this event is the subject of significant uncertainty
4
5 91 | and debate, with a majority of studies considering it to be ~~eaca.~~ 2490 - 2480 Ma (e.g., Corfu
6
7 92 | et al. 1994; Love et al., 2004; Goodenough et al., 2013). Others (e.g., Friend and Kinny
8
9 93 | 1995; Kinny and Friend, 1997) suggest that the Inverian is a younger – as yet undated –
10
11 94 | event younger than ~~eaca.~~ 2480 Ma while still pre-dating the oldest Scourie dykes. These
12
13 95 | mafic to ultramafic Scourie dykes are found throughout the Assynt Terrane, ranging in
14
15 96 | thickness from a few mm to several tens of m and were intruded ~~eaca.~~ 1900 - 2400 Ma (Rb-
16
17 97 | Sr whole rock and U-Pb geochronology; Chapman 1979; Heaman & Tarney, 1989; Davies &
18
19 98 | Heaman 2014³). The NW-SE-trending Scourie dykes cross-cut local Inverian fabrics and
20
21 99 | display evidence of having been emplaced under amphibolite facies pressures and
22
23 100 | temperatures, i.e. in the middle crust, possibly immediately following the Inverian event
24
25 101 | (O'Hara, 1961; Tarney, 1973; Wheeler et al., 2010).

26
27 102 | In the Assynt Terrane, the significantly later main phase Laxfordian event has
28
29 103 | traditionally been associated with the shearing of the Scourie dykes and widespread
30
31 104 | retrogression of the TTG gneisses under lower amphibolite to upper greenschist-facies
32
33 105 | metamorphic conditions (e.g., Sutton and Watson, 1951; Attfield, 1987; Beacom et al.,
34
35 106 | 2001). The Laxfordian is recognised throughout much of the Lewisian complex and appears
36
37 107 | to be a long lived series of events starting with a series of magmatic events ~~eaca.~~ 1900-1870
38
39 108 | Ma – at least some of which are related to island arc development – followed by a protracted
40
41 109 | orogenic episode lasting from 1790 - 1660 Ma (see discussion in Goodenough et al., 2013).
42
43 110 | The effects of Laxfordian reworking in the Assynt Terrane are highly localised, being largely
44
45 111 | restricted to the central part (~~eaca.~~ 1km wide) of the CSZ and other shear zones, as well as
46
47 112 | along the margins of the Scourie dykes. This contrasts with the neighbouring Rhiconich and
48
49 113 | Gruinard Terranes where the Laxfordian event reached amphibolite facies and was
50
51 114 | associated with more pervasive ductile shearing and reworking (Droop et al., 1989). This has
52
53 115 | led to the suggestion that the Assynt Terrane represents a shallower depth crustal block
54
55 116 | during the Laxfordian (e.g., Dickinson and Watson, 1976; Coward and Park, 1987).
56
57
58
59
60
61
62
63
64
65

1
2
3 117 In the Assynt and Guinard terranes, a younger set of 'late Laxfordian' sinistral low
4
5 118 greenschist-facies mylonitic shear zones, brittle faults and localized folds is recognised
6
7 119 developed sub-parallel to the pre-existing high-strain fabrics in Laxfordian and Inverian shear
8
9 120 zones (see Beacom et al. 2001). These structures include the Loch Assynt Fault (Fig. 1).
10
11 121 The precise age of the 'late-Laxfordian' faulting is poorly constrained, but these structures
12
13 122 are unconformably overlain by the unmetamorphosed and little deformed ca. 1200 Ma
14
15 123 Torridonian Stoer Group. This suggests that the presently exposed parts of the Lewisian
16
17 124 Complex had been exhumed to the surface by ca. 1200 Ma. Regionally, both the Stoer
18
19 125 Group and the Lewisian Complex are unconformably overlain by younger Torridonian
20
21 126 sequences (Diabeg and Torridon groups) thought to have been deposited no earlier than 1.1
22
23 127 Ga (Park et al. 1994).

25 129 *Lewisian host rocks*

26
27 130 The Badcallian amphibolite- to granulite-facies TTG gneisses of the Assynt Terrane show
28
29 131 foliation development on all scales (e.g., Fig 2a), from millimetres to tens of metres (e.g.
30
31 132 Sheraton et al., 1973). The foliation is best developed in intermediate composition gneisses,
32
33 133 where it is defined by 0.5 to 5 cm thick layers of contrasting light (plagioclase and quartz)
34
35 134 and dark (pyroxene, hornblende and biotite) layers, with individual layers rarely continuing
36
37 135 for more than a few metres (Jensen, 1984). Representative samples from the Loch Assynt
38
39 136 area typically contain 30% quartz, 20% plagioclase, 10% microcline, 10% orthopyroxene and
40
41 137 30% heavily retrogressed clinopyroxene. Relict grains of the latter mineral are replaced by
42
43 138 fine grained intergrown aggregates of chlorite, epidote, actinolite and hornblende.

44
45 139 The Badcallian gneisses were reworked in dextral-reverse shear zones (e.g., the
46
47 140 CSZ) during the Inverian, which imposed a NW-SE foliation in the rocks, mainly by
48
49 141 reorientation and attenuation of the pre-existing gneissose foliation (e.g., Fig. 2b; Attfeld,
50
51 142 1987). Deformation within the Inverian shear zones is extremely heterogeneous, with
52
53 143 lenses of lower-strain, more massive material enclosed by anastomosing bands of highly
54
55 144 deformed, sheared gneiss (e.g., Attfeld, 1987; Chattopadhyay et al., 2010). Representative
56
57
58
59
60
61
62
63
64
65

1
2
3 145 samples of reworked Inverian gneisses from within the CSZ contain 20% quartz, 40%
4
5 146 feldspar (predominantly plagioclase with alteration bands), 5% pyroxene, 15% hornblende,
6
7 147 15% biotite and chlorite, and 5% other minerals such as epidote. The hornblende, epidote,
8
9 148 biotite and chlorite are likely to be a product of the breakdown and hydration of pyroxenes
10
11 149 during retrogression (Beach, 1976). The quartz crystals contain 0.25 - 1mm subgrains and
12
13 150 form irregular, sub-parallel ribbons of crystals, which are smaller than in the undeformed
14
15 151 Badcallian gneisses, possibly due to syn-tectonic recrystallisation (Jensen, 1984).

16 152 The Laxfordian event reactivated the central part of the CSZ with a dextral shear
17
18 153 sense, producing a new, finer foliation (e.g., Fig. 2d; Sheraton et al., 1973; Attfield, 1978).
19
20 154 Commonly, the reworked rocks in both small and large shear zones have a mineralogy that
21
22 155 differs significantly from that of the original gneiss and the extent of the changes that occur
23
24 156 appears to be in proportion to the intensity of the deformation (e.g., see Beach, 1976). A
25
26 157 typical sample of Laxfordian-deformed gneiss from the CSZ contains 75% quartz, 10%
27
28 158 hornblende, 10% biotite and muscovite, and 5% feldspar porphyroblasts (typically ~1mm in
29
30 159 size). The quartz is banded on a millimetre scale with alternating bands of small quartz
31
32 160 grains (<100µm) and larger quartz grains (~500µm to 1mm) which form an anastomosing
33
34 161 schistose foliation (Jensen, 1984). Quartz grain boundaries are often pinned by aligned
35
36 162 micas and layers richer in mica therefore tend to show finer quartz grain sizes compared to
37
38 163 mica-poor layers. The quartz crystals themselves are often elongate and contain poorly
39
40 164 developed subgrains. Petrographic observations of Lewisian gneisses show that during
41
42 165 regression, pyroxene is first replaced by hornblende which is then replaced by biotite in the
43
44 166 most intensely deformed gneisses (Beach, 1976). The Laxfordian reworking occurred in
45
46 167 intense zones which anastomose around relict lenses of Badcallian or Inverian gneiss
47
48 168 (Sheraton et al., 1973). Tight intrafolial folds are common within the Laxfordian-deformed
49
50 169 gneisses and, in places, Inverian folds have been refolded (e.g. on the coast at Port Alltan
51
52 170 na Bradhan; see Attfield, 1987; Chattopadhyay et al., 2010). The Scourie dykes within and
53
54 171 adjacent to the CSZ have also been pervasively affected by Laxfordian reworking with
55
56
57
58
59
60
61
62
63
64
65

1
2
3 172 shearing particularly concentrated along their margins (Sheraton et al., 1973). Most dykes in
4
5 173 the CSZ are sheared into near concordance with the surrounding foliation in the gneisses.
6
7 174

8 9 175 **3. Field and Laboratory Methods**

10 176 *3.1. Fieldwork*

11
12 177 Fieldwork was carried out visiting well-exposed examples of quartz-pyrite vein localities in
13
14 178 the Assynt Terrane and in one area of the Gruinard Terrane (Fig. 1). The relative ages of
15
16 179 country rock fabrics and veins were determined at 83 locations using cross-cutting
17
18 180 relationships and the orientations of both veins and fabrics were measured. Representative
19
20 181 (orientated) hand samples of both country rocks and veins were taken at a number of key
21
22 182 localities in order to study deformation microstructures using an optical microscope and also
23
24 183 to extract fresh samples of pyrite for Re-Os dating. Having separated appropriate material
25
26 184 for dating, we used Re-Os geochronology to determine the age of sulphide (pyrite)
27
28 185 mineralization present in several of the quartz veins. We additionally determined sulphur
29
30 186 isotope compositions of the dated samples to yield evidence of the origin of the sulphur and
31
32 187 by inference the hydrothermal fluids associated with the quartz-pyrite vein formation.
33

34 189 *3.2. Rhenium-Osmium Geochronology Analytical Methods*

35
36 190 Six pyrite samples co-genetic with quartz veining were analyzed for their rhenium (Re) and
37
38 191 osmium (Os) abundances and isotopic compositions. The analyses were conducted at the
39
40 192 TOTAL Laboratory for Source Rock Geochronology and Geochemistry at Durham
41
42 193 University. The pyrite sample set was collected from five locations: four in the Assynt
43
44 194 Terrane and one in the Gruinard Terrane (Fig. 1; Table 1).

45 195 The pyrite samples were isolated from the vein host material by crushing, without
46
47 196 metal contact, to a < 5 mm grain size. After this stage > 1 g of pyrite was separated from the
48
49 197 crushed vein by hand picking under a microscope to obtain a clean mineral separate. The
50
51 198 Re and Os analysis reported in this study followed the analytical protocols of Selby et al.
52
53 199 (2009). In brief, this involved loading ~ 0.4 g of accurately weighed pyrite into a carius tube
54
55
56
57
58
59
60
61
62
63
64
65

1
2
3 200 with a known amount of a ^{185}Re and ^{190}Os tracer (spike) solution and 11 ml of inverse *aqua*
4
5 201 *regia* (3 ml 11N HCl and 8 ml 15 N HNO_3). The carius tubes were then sealed and placed in
6
7 202 an oven at 220°C for 48 hrs. Osmium was isolated and purified from the acid medium using
8
9 203 CHCl_3 solvent extraction and micro-distillation, with Re separated by anion exchange column
10
11 204 and single-bead chromatography. The Re and Os fractions were then loaded onto Ni and Pt
12
13 205 filaments, respectively, and analyzed for their isotope compositions using negative-ion mass
14
15 206 spectrometry on a Thermo Electron TRITON mass spectrometer. Rhenium isotopes were
16
17 207 measured statically using Faraday Collectors, with the Os measured in peak hopping mode
18
19 208 using the Secondary Electron Multiplier. Total procedural blanks for Re and Os are 2.7 ± 1.1
20
21 209 pg and 0.4 ± 0.4 pg, respectively, with an average $^{187}\text{Os}/^{188}\text{Os}$ of 0.37 ± 0.17 ($n = 2$, 1 SD).
22
23 210 The Re and Os uncertainties presented in Table 1 are determined by the full propagation of
24
25 211 uncertainties from the mass spectrometer measurements, blank abundances and isotopic
26
27 212 compositions, spike calibrations, and the results from analyses of Re and Os standards. The
28
29 213 Re standard data together with the accepted $^{185}\text{Re}/^{187}\text{Re}$ ratio (0.59738; Gramlich et al.,
30
31 214 1973) are used to correct for mass fractionation. The Re and Os standard solution
32
33 215 measurements performed during the two mass spectrometry runs were 0.5982 ± 0.0012
34
35 216 (Re std, $n = 2$) and 0.1608 ± 0.0002 (DROsS, $n = 2$), respectively, which agree with the
36
37 217 values reported by Finlay et al. (2011) and references therein.

38 218 3.3. Sulphur Isotope Analytical Protocol

39
40 219 Aliquants of pyrite samples for sulphur isotope analysis were taken from the quartz veins at
41
42 220 the same five locations as those used for the Re-Os geochronology (Table 1). Approximately
43
44 221 0.01g was used for the analysis, with the sulphur extracted as SO_2 from the pyrite by fusing
45
46 222 the sample under vacuum at 1076°C in a Cu_2O (200mg) matrix (Wilkinson & Wyree et al.,
47
48 223 2005). ~~The method of Coleman & Moore (1973) was followed for extracting sulphur from~~
49
50 224 ~~SO_2 from sulphates and. The sample was then~~ analysed on a VG SIRA II mass
51
52 225 spectrometer to obtain values for $\delta^{66}\text{SO}_2$ which were converted to $\delta^{34}\text{S}$. Standard correction
53
54 226 factors were applied (Craig, 1957). Results are given in conventional $\delta^{34}\text{S}$ notation relative to
55
56
57
58
59
60
61
62
63
64
65

1
2
3
4
5
6
7
8
9
10
11
12
13
14
15
16
17
18
19
20
21
22
23
24
25
26
27
28
29
30
31
32
33
34
35
36
37
38
39
40
41
42
43
44
45
46
47
48
49
50
51
52
53
54
55
56
57
58
59
60
61
62
63
64
65

228 the Vienna Canon Diablo troilite standard (V-CDT). The reproducibility based on full replicate
229 analyses of internal laboratory standards was ± 0.2 per mil (1σ).

231 4. Field relationships of the quartz-pyrite veins

232 The occurrence of quartz veins is a widely recognised, but little described phenomenon in
233 the rocks of the Assynt Terrane (e.g., the presence of quartz veins is noted in Sheraton et
234 al., 1973). Some generally foliation-parallel veins are clearly relatively late features that are
235 closely associated with shearing along Laxfordian shear zones and the development of
236 schistose, phyllosilicate-rich high strain zones (e.g., Beach, 1976; Beacom, 1999). However,
237 the present study has revealed that an earlier, much more widespread and distinctive group
238 of quartz-pyrite veins are present throughout the Assynt Terrane and at least part of the
239 Gruinard Terrane. The distribution of the quartz veins does not seem uniform – they typically
240 occur in clusters cutting the gneisses in regions covering areas of tens to hundreds of
241 square metres, with particularly well-defined groups recognised in the Loch Assynt and
242 Clashnessie regions of the Assynt Terrane, and along the trace of the CSZ (Fig. 1).

243 The quartz veins typically range in thickness from a few millimetres to several tens of
244 centimetres (e.g., Fig. 2a-e, g), and are relatively straight and continuous features that can
245 be traced for several metres or, less commonly, tens of metres along strike. They have
246 sharply-defined margins, are occasionally anastomosing and sometimes contain inclusions
247 of country-rock or clusters of pink K-feldspar. Pyrite is not found in all of the veins, but where
248 it occurs it is typically either located along the margins as large crystals (>0.5 mm) or as
249 large clusters (>1 cm) of crystals distributed sparsely throughout the veins (e.g., Fig. 2h). In
250 some cases pyrite clusters have been partially to completely oxidised to hematite or limonite,
251 particularly where they have been exposed at the surface for an extended period; this often
252 gives weathered veins a distinctive localised orange-red staining. Within the CSZ, pyrite
253 crystals are also sometimes found in the sheared gneisses surrounding the vein. In isolated
254 road cut exposures, the development of quartz-pyrite veins is additionally associated with a

1
2
3 255 localised yellow-brown sulphurous weathering of the gneisses, e.g., in roadcuts east of
4
5 256 Lochinver (National grid reference NC 1012 2366; Samples BH2 and 5; Table 1).
6
7 257

8
9 258 *4.1. Cross-cutting relationships*

10 259 The quartz-pyrite veins display a consistent set of cross-cutting relationships with other
11
12 260 features in the Lewisian Complex. They typically cross-cut the oldest, moderately to
13
14 261 shallowly-dipping Badcallian foliations and folds (e.g., Fig. 2a), although in areas where the
15
16 262 foliation is particularly intense and of variable orientation (e.g. Clashnessie), the veins may
17
18 263 locally be concordant with the local foliation. The veins also consistently cross-cut the
19
20 264 steeply-dipping Inverian shear fabrics of the CSZ (e.g., Fig. 2b) and other minor shear zones
21
22 265 of this age within the terrane, as well as all observed Scourie dykes (e.g., Fig. 2c). Both
23
24 266 veins and dykes are consistently overprinted and reworked by dextral shear fabrics related
25
26 267 to the Laxfordian event, including the development of the central part of the CSZ (Attfield
27
28 268 1987; e.g., Fig. 2d). The quartz veins are also post-dated by 'late Laxfordian', epidote-
29
30 269 bearing small-scale shear zones and fractures, which exhibit a predominantly sinistral sense
31
32 270 of shear (e.g., Fig. 2e, f; see Beacom et al 2001). Many of the larger quartz vein clasts found
33
34 271 in the immediately overlying basal units of the Torridonian sandstones are plausibly derived
35
36 272 from the basement veins. The quartz-pyrite veins are everywhere cross-cut by gouge-
37
38 273 bearing Phanerozoic (post-Cambrian) normal faults (e.g., NC 1020 2360).

38 274 Thus the field observations suggest that the quartz-pyrite veins post-date Badcallian
39
40 275 structures, the NW-SE trending Inverian fabrics and Scourie dykes. They appear to pre-date
41
42 276 all Laxfordian fabrics, 'late Laxfordian' faults, the deposition of the Torridonian sediments
43
44 277 and all post-Torridonian deformation episodes (mainly faulting).
45
46 278

47 279 *4.2. Orientation and kinematics*

48
49 280 The orientations of 140 quartz-pyrite veins measured in the Assynt Terrane during the
50
51 281 present study are shown in Figures 3a-c, and the sparse lineations found on the veins in
52
53 282 Figure 3aii. A rose diagram plot (Fig. 3ai) suggests a predominance of NE-SW strikes with
54
55
56
57
58
59
60
61
62
63
64
65

1
2
3 283 subordinate NW-SE trends. The regional stereograms (Figs. 3biv-vi & c) better illustrate the
4
5 284 rather wider range of vein orientations, with a reasonably strong concentration of planes
6
7 285 striking NE-SW and, to a lesser extent NW-SE. Both sets display bimodal dip directions
8
9 286 (e.g., NW or SE and NE or SW, respectively; Figs. 3biv-vi & c). These observations suggest
10
11 287 a generally multimodal pattern of fracture orientations.

12 288 In order to investigate the possible effects on vein orientation of local country rock
13
14 289 fabrics and Laxfordian overprinting, the data have been plotted according to the age of the
15
16 290 local fabrics they cross-cut or are reworked by (Fig. 3b). In the regions of gneiss dominated
17
18 291 by the Badcallian event, both the foliations (Fig. 3bi) and the veins (Fig. 3biv) have large
19
20 292 variations in their orientations. The foliation shows a poorly-defined N-S trend dipping
21
22 293 shallowly W, whereas the veins show a reasonably strong NE-SW trend, with bimodal dips
23
24 294 steeply to the NW and rather more shallowly to the SE. The Inverian foliation has a strong
25
26 295 NW-SE trend with generally steep dips (Fig. 3bii), whereas the veins show a strong NE-SW
27
28 296 trend with dips mainly being steep and to the NW (Fig. 3bv). Both the Laxfordian foliation
29
30 297 and the veins within the Laxfordian fabrics show a strong NW-SE trend and steep dips (Figs.
31
32 298 3biii and vi), reflecting the strong reworking and reorientation of veins into parallelism with
33
34 299 those fabrics during overprinting deformation.

35
36 300 The data have also been plotted according to the localities where well-defined
37
38 301 clusters of veins are found (Figs. 3ci-vi). The stereoplots for localities such as Clashnessie
39
40 302 and Achmelvich areas (Figs. 3ci-ii) show a wide range of orientations whilst the best defined,
41
42 303 statistically significant trend is found in the Loch Assynt cluster (Fig. 3cv). Here there is a
43
44 304 very well-defined trend striking NE-SW with the majority of veins dipping steeply NW. It may
45
46 305 be significant that the pre-vein Badcallian foliation in this area is much weaker compared to
47
48 306 areas such as Clashnessie.

49 307 The kinematics of the quartz veins are difficult to deduce with any precision. Most of
50
51 308 the veins appear to be dilational (Mode 1 tensile) features based on observed offsets of
52
53 309 markers in the adjacent wall rocks, i.e., the vein opening directions lie at high angles to the
54
55 310 vein walls). A few large veins in the Loch Assynt and Lochinver regions display regular en
56
57
58
59
60
61
62
63
64
65

Formatted: Font: Not Bold

1
2
3 311 echelon off-shoots (e.g., Fig. 2g) consistent with some degree of vein-parallel shearing
4
5 312 during emplacement (e.g. Peacock & Sanderson 1995). Of the seven veins found with such
6
7 313 off-shoots, five indicated a sinistral and two a dextral sense of shear. There does not appear
8
9 314 to be any obvious orientation control on the shearing directions, suggesting the shearing
10
11 315 may be due to local strain heterogeneities. A few veins (n = 7) unaffected by Laxfordian
12 316 reworking display poorly developed mainly oblique mineral lineations on their outer contacts
13
14 317 (Fig. 3a_{ii}).
15

17 318 18 319 **56. Rhenium-Osmium Geochronology**

19 320 The total Re and Os abundances of the pyrite samples range from 6.8 to 25.8 ppb (parts per
20
21 321 billion) and 298.8 to 660.5 ppt (parts per trillion; Table 1), respectively. The majority of the
22
23 322 Os within the samples is radiogenic ^{187}Os (> 92 %). Four of the samples possess > 99 %
24
25 323 radiogenic ^{187}Os (Table 1). As a result, the $^{187}\text{Re}/^{188}\text{Os}$ values are high to very high (265.6 to
26
27 324 17531), with the accompanying $^{187}\text{Os}/^{188}\text{Os}$ values being very radiogenic (11.04 to 675.2).
28
29 325 The predominance of radiogenic ^{187}Os ($^{187}\text{Os}^r$) in the pyrite samples defines them as Low
30
31 326 Level Highly Radiogenic (LLHR; Stein et al., 2000; Morelli et al., 2005). To account for the
32 327 high-correlated uncertainties between the $^{187}\text{Re}/^{188}\text{Os}$ and $^{187}\text{Os}/^{188}\text{Os}$ data we present the
33
34 328 latter with the associated uncertainty correlation value, ρ (Ludwig, 1980), and the 2σ
35
36 329 calculated uncertainties for $^{187}\text{Re}/^{188}\text{Os}$ and $^{187}\text{Os}/^{188}\text{Os}$ (Table 1). The regression of all the
37
38 330 Re-Os data using *Isoplot V. 3.0* (Ludwig, 2003) and the ^{187}Re decay constant (λ) of
39
40 331 $1.666 \times 10^{-11} \text{a}^{-1}$ (Smoliar et al., 1996) yields a Model 3 Re-Os age of 2259 ± 61 (2.9 %) Ma,
41
42 332 with an initial $^{187}\text{Os}/^{188}\text{Os}$ of 0.9 ± 9.0 (2σ , Mean Squared Weighted Deviates [MSWD] = 22;
43
44 333 Fig. 5a). Although the calculated Re-Os age has only a 2.9 % uncertainty, the high MSWD
45 334 value (22) suggests that the degree of scatter about the regression line is a function of pyrite
46
47 335 Re-Os systematics (discussed below). The imprecision of the initial $^{187}\text{Os}/^{188}\text{Os}$ does not
48
49 336 permit an accurate evaluation of the origin of the Os in the pyrite, however the initial
50
51 337 $^{187}\text{Os}/^{188}\text{Os}$ value, including the uncertainty, can be used to calculate the abundance of
52
53
54
55
56
57
58
59
60
61
62
63
64
65

Fig. 5c). In summary, the ages determined from both the Re-Os isochron methods and the weighted average of the Re-Os model ages are all within uncertainty. We favour using the $^{187}\text{Re}/^{188}\text{Os}$ vs $^{187}\text{Os}/^{188}\text{Os}$ isochron age (without sample 64-1). From this study we consider the majority of the pyrite mineralization and by inference the precipitation the quartz pyrite veins and fracture formation occurred at 2249 ± 77 Ma.

67. Sulphur Isotope Analysis

All the samples from the sulphur isotope analysis yielded high amounts of sulphur (82 to, 97% yield). The $\delta^{34}\text{S}$ from the sulphides ranges from +3.0 to -2.2 per mil. All the samples are slightly enriched in ^{34}S relative to 0 per mil, with the exception of sample 64.1, which has a slightly depleted value of -2.2. This may suggest a slightly different source of the sulphur for sample 64.1, and coupled with the Re-Os data may support a distinct quartz and pyrite mineralization event from the other five samples. The range in the $\delta^{34}\text{S}$ values (+3.0 and -2.2) encompasses that of the primitive mantle (Rollinson, 1993). The results therefore suggest that the sulphur in the pyrite is most likely derived from a source not isotopically fractionated from the primitive mantle valuesource.

75. Microstructural textures and inferred deformation mechanisms

75.1. Microstructural textures within quartz-pyrite veins

The quartz-pyrite veins display an array of deformation textures suggesting that they have experienced a complex history of deformation at different temperatures and pressures. A number of overprinting relationships are seen which can be related to the relative chronology of events seen in the field. The deformation textures are described below with reference to the age of the country rock fabric which the veins either cross-cut or are overprinted by.

75.1.1 Veins crosscutting Badcallian structures

1
2
3 391 Despite modest amounts of grain-scale deformation, the veins cross-cutting Badcallian
4
5 392 gneisses (e.g., Fig. 2a, e) preserve a diverse range of deformation microstructures. The
6
7 393 most deformed examples contain large quartz crystals (> 1mm, but typically 3 – 7mm) that
8
9 394 show sweeping undulose extinction and have highly lobate grain boundaries as a result of
10
11 395 grain boundary migration processes during recrystallisation (Stipp et al., 2002). Chessboard
12
13 396 subgrains (e.g. Fig. 4a) within quartz crystals are also common and form in response to the
14
15 397 migration of dislocations within the crystal lattice into subgrain walls during recrystallisation
16
17 398 (e.g. Passchier and Trouw, 2005).

18 399 The least plastically deformed veins cutting Badcallian foliation are found on the
19
20 400 shores of Loch Assynt (e.g., Figs. 2e, g). The quartz crystals within these veins display
21
22 401 undulose extinction, whilst some larger grains contain deformation lamellae, which are zones
23
24 402 of differently orientated crystal lattice separated by dislocations. Grain boundaries have
25
26 403 undergone small-scale bulging during recrystallisation and small grains (<100µm) have
27
28 404 developed within the bulges and along the deformation lamellae (e.g., Fig. 4b).

29 405 Overall, the range of deformation microstructures observed in the quartz veins cutting
30
31 406 Badcallian gneisses suggests that they experienced small amounts of crystal plastic
32
33 407 deformation under moderate temperature (400 - 500°C) conditions. The veins on the shore
34
35 408 of Loch Assynt locally preserve rather lower temperatures textures (perhaps as low as
36
37 409 300°C) and/or higher strain rate conditions. This may be the result of 'late Laxfordian'
38
39 410 deformation associated with slip on the Loch Assynt Fault (e.g., like the structures shown in
40
41 411 Figs. 2e, f), to which they are proximal.

43 413 **7.5.1.2** Veins cross-cutting Inverian structures

44
45 414 Veins emplaced into Lewisian gneisses reworked by Inverian deformation (e.g., Fig. 2b) also
46
47 415 show little obvious deformation at outcrop scale. A range of deformation microstructures are
48
49 416 preserved, including undulose extinction, deformation lamellae, new grain growth along
50
51 417 crystal boundaries, subgrain development and the development of lobate grain boundaries.
52
53 418 These are indicative of recrystallisation under low to moderate temperatures (350 - 500°C)

1
2
3 419 and high to moderate strain rates. Some veins contain large (>2mm) quartz crystals with
4
5 420 lobate boundaries, formed by grain boundary migration under moderate temperatures and
6
7 421 strain rates, which show grain boundary bulging and the development of new, small grains
8
9 422 (<250µm) within the bulges, particularly at triple-point grain boundaries (Fig. 4c). These
10
11 423 structures are typical of recrystallisation under somewhat lower temperatures (300 - 400°C),
12
13 424 and may indicate a lower temperature event. There is little evidence for this event within the
14
15 425 veins emplaced into Badcallian gneisses, and it may be that it is related to localised later
16
17 426 deformation and/or fluid flow restricted to the Inverian shear zones immediately following
18
19 427 vein emplacement. Alternatively, it may be a weak manifestation of Laxfordian deformation
20
21 428 given the regionally observed coincidence of Inverian and Laxfordian reworking (e.g. Attfeld
22
23 429 | 1987).

25 431 | **7.5.1.3** Veins overprinted by Laxfordian structures

26
27 432 The veins emplaced within the Laxfordian part of the CSZ (e.g., Fig. 2d) have been heavily
28
29 433 reworked at outcrop scale. Many of the grain-scale textures resulting from the
30
31 434 recrystallisation of quartz are similar to those seen in the veins which were emplaced into
32
33 435 gneisses with Badcallian and Inverian foliations, but the finite strains are much higher. In
34
35 436 most veins, larger quartz crystals (>2mm) show sweeping undulose extinction, deformation
36
37 437 lamellae, subgrain development and lobate grain boundaries. These microstructures indicate
38
39 438 deformation under moderate temperatures (350 - 500°C) and strain rates. Relict S-C'
40
41 439 mylonite fabrics (e.g. Berthé et al. 1979; Snoke et al. 1998) are preserved in the most highly
42
43 440 | deformed veins (e.g., Fig. 4d). Sub-parallel fine-grained (<100 µm) bands of feldspar,
44
45 441 muscovite and chlorite define the C-surfaces which are enclosed by polygonal quartz
46
47 442 aggregate (with grains sizes 0.5 – 3 mm). Quartz grain boundaries are often pinned by
48
49 443 aligned micas and some fine aligned grains are completely enclosed by much larger,
50
51 444 undeformed quartz grains (Fig. 4d). These fabrics are typical indicators of significant
52
53 445 secondary grain growth under elevated temperature conditions (e.g., Vernon 1976;
54
55 446 Passchier and Trouw, 2005).
56
57
58
59
60
61
62
63
64
65

1
2
3 447
4
5 448
6
7 449
8
9 450
10
11 451
12
13 452
14
15 453
16
17 454
18
19 455
20
21 456
22
23 457
24
25 458
26
27 459
28
29 460
30
31 461
32
33 462
34
35 463
36
37 464
38
39 465
40
41 466
42
43 467
44
45 468
46
47 469
48
49 470
50
51 471
52
53 472
54
55 473
56
57 474
58
59
60
61
62
63
64
65

75.1.4 Pyrite microstructural relationships

Pyrite occurs in a variety of forms in the veins of the Assynt Terrane. Some samples contain large clusters of pyrite crystals up to 1.5cm in across (e.g., Fig. 2h) which are intimately intergrown with quartz (e.g., Figs 4e, f). SEM images reveal the partial alteration of pyrite grains to iron oxides along grain margins and fractures within some large pyrite clusters (e.g., Fig. 4g, h). Small (<1mm) pyrite clusters are also associated with the mylonitized quartz veins within the CSZ. There is little evidence for significant deformation of the pyrite grains during recrystallization of the surrounding quartz aggregates even in cases where the intensity of finite plastic strain is high.

75.1.5 Summary

The microstructural evidence from the veins suggests that most of the pyrite initially crystallised at the same time as the quartz and that it is therefore a primary mineral phase. The veins then experienced very modest amounts of deformation and recrystallisation during a moderate temperature (350 - 500°C) and low strain rate strain rate event felt throughout most of the Assynt Terrane. Given the similarity in quartz microstructures and interpreted palaeotemperatures with the more highly deformed veins in the CSZ, it seems most likely that the bulk of the modest deformations recorded here are also Laxfordian to 'late Laxfordian' in age (ca. 1780-1400). Laxfordian deformation, especially within the CSZ, resulted in the formation of mylonitic fabrics within the veins under mostly moderate temperatures (350 - 500°C). There may also have been some limited remobilisation and re-precipitation of pyrite related to fluid flow both within the veins and the adjacent sheared gneisses.

8. Discussion:

The Re-Os isochron age obtained from the majority of the quartz-pyrite veins (2249 ± 77 Ma) is consistent with our current understanding of the broad ages of regional

1
2
3 475 tectonometamorphic episodes in the Lewisian Complex (Fig. 6). Specifically, they cross cut
4
5 476 older Badcallian (*ca.* 2760 or 2480 Ma) and Inverian (*ca.* 2400-2480 Ma) fabrics and are
6
7 477 overprinted/reworked by younger Laxfordian (1790-1660 Ma) structures. The latter suggests
8
9 478 that the Re-Os systematics were not appreciably disturbed by structural reworking and the
10
11 479 upper greenschist conditions associated with the Laxfordian event.

12 480 The most recent U-Pb geochronology shows that intrusion of the Scourie dykes
13
14 481 predominantly occurred at 2391 – 2404 Ma, with moderately younger ages (2367 – 2372
15
16 482 Ma) at the SW edge of the Assynt Terrane (Davies and Heaman, 2014³). The *ca.* 2250 Ma
17
18 483 age for the quartz-pyrite veins falls within the range of ages obtained from the NW-SE
19
20 484 trending Scourie dyke swarm across the entire Lewisian Complex (Fig. 6; 2418 Ma to 1991
21
22 485 Ma; Chapman 1979; Heaman and Tarney, 1989; Cohen et al., 1988; Waters et al., 1990;
23 486 Davies and Heaman, 2014³). These studies suggest two main episodes of dyke intrusion at
24
25 487 *ca.* 2418 Ma and 1992 Ma (Fig. 6; Davies and Heaman, 2014³), with distinct mantle sources
26
27 488 exploited during each event (Cartwright and Valley, 1991). The idea that there are multiple
28
29 489 episodes of 'Scourie dyke's intrusion is consistent with some geological field relationships. It
30
31 490 is known, for example, in the southern region of the Lewisian Complex that some 'Scourie
32 491 dykes' cut the Loch Maree Group metasediments and metavolcanics, which were thought to
33
34 492 have formed in oceanic basins and accreted to the continental crust through subduction
35
36 493 between 2000 and 1900 Ma (Park et al., 2001).

37
38 494 All the quartz-pyrite veins observed during the present study seen in the Assynt
39
40 495 Terrane cross-cut Scourie dykes, although this does not preclude the possibility that
41
42 496 regionally there may be some dykes that are younger. However, the Re-Os pyrite dating of
43 497 the veins at *ca.* 2250 Ma suggests a complex polyphase early Palaeoproterozoic tectonic
44
45 498 history of the Lewisian complex (Fig. 6). Veins form by the precipitation of minerals in dilating
46
47 499 hydrofractures and their regional development in clusters and swarms are indicative of
48
49 500 significant phase of ~~crustal-scale~~ fluid flow in the crust (e.g., Sibson, 1996 and references
50
51 501 therein). The simplest types of vein are Mode 1 fractures which open in the direction of the
52 502 minimum principle stress and have strike orientations perpendicular to it (e.g., Peacock &
53
54
55
56
57
58
59
60
61
62
63
64
65

Formatted: Font: Italic

Formatted: Font: Italic

Formatted: Font: Italic

Formatted: Font: Italic

Formatted: Font: Italic

1
2
3 503 Mann, 2005). Most of the veins in the Assynt Terrane appear on the basis of their field
4
5 504 relationships to be Mode I features (e.g. Fig. 2a). If so, the prevalence of NE-SW strikes
6
7 505 (e.g., Figs. 1, 3ai) implies a NW-SE opening direction, although the veins show a wide range
8
9 506 of other orientations (Figs. 3b,c) which are attributed to a number of factors: the presence of
10
11 507 highly variable foliation in strongly banded gneisses; the presence of pre-existing fractures,
12
13 508 or to the reworking of veins by Laxfordian fabrics.

14 509 The pre-Laxfordian NE-SW orientation and inferred NW-SE opening directions of the
15
16 510 quartz-pyrite veins lie almost orthogonal to the regional NW-SE orientation – and inferred
17
18 511 NE-SW extension direction - of the Scourie dykes. If there are multiple episodes of Scourie
19
20 512 dykes on a regional scale, with some pre-dating and some post-dating the quartz-pyrite
21
22 513 veins, this implies that there were significant changes in the orientation of regional stress
23
24 514 vectors in the 500 Ma period between 2400 and 1900 Ma (Fig. 6). Note, however, that in
25
26 515 common with the Scourie dykes, the sulphur isotopic analysis of the quartz-pyrite veins is
27
28 516 suggestive of a source not isotopically fractionated from the primitive mantle derivation
29
30 517 value~~Note, however, that in common with the Scourie dykes, the sulphur isotopic analysis of~~
31
32 518 ~~the quartz-pyrite veins is suggestive of a primitive mantle derivation~~ (Rollinson, 1993).

32 519 Although tThe Re-Os ~~model agedata for-of~~ sample 64.1 provide a highly imprecise
33
34 520 model age (1597.6 ± 1356 Ma) its nominal age is considerably younger than the model ages
35
36 521 for the other samples (2198.5 – 2328.7 Ma), and, in addition, has a very large uncertainty as
37
38 522 well as the lowest Os abundance of (242.8 ± 33.9 ppb) of all the samples; ~~it~~. Furthermore,
39
40 523 sample 64.1 is also the only sample with a depleted $\delta^{34}\text{S}$ value (-2.2). Although this value
41
42 524 could indicate that the sulphur source is not isotopically fractionated from the primitive mantle
43
44 525 value is derived from the primitive mantle, like the other samples, it may be that the
45
46 526 sulphur ~~uride~~ within the vein-pyrite has a slightly different origin to that found within other veins,
47
48 527 or that it may have been disturbed following emplacement, perhaps related to a later phase
49
50 528 of 'late Laxfordian' brittle fracture fractures and fluid ingress. Further work and dating is
51
52 529 required to verify the age obtained and better constrain the geological and geochronological
52
53 530 significance of this younger age.

1
2
3 531
4
5 532
6
7 533
8
9 534
10
11 535
12
13 536
14
15 537
16 538
17
18 539
19
20 540
21
22 541
23 542
24
25 543
26
27 544
28
29 545
30
31 546
32
33 547
34
35 548
36 549
37
38 550
39
40 551
41
42 552
43
44 553
45
46 554
47
48 555
49 556
50
51 557
52
53
54
55
56
57
58
59
60
61
62
63
64
65

86.1. Implications for terrane models

Dating of the TTG protoliths suggests that the gneisses of the Gruinard Terrane are at least 100 Ma younger than those of the Assynt Terrane and underwent granulite metamorphism at 2730 Ma (Love et al., 2004; Park, 2005). Thus they are thought to belong to different and separate Archaean terrane which amalgamated along the Strathan Line, south of Lochinver, during Inverian folding and retrogression (Fig. 1, Love et al., 2004). The presence of post-Inverian quartz-pyrite veins within both the Assynt and Gruinard Terranes is consistent with this proposal.

The amphibolite-facies gneisses of the Rhiconich Terrane to the north have yielded protolith ages of 2840-2800 Ma and a record magmatism at 2680 Ma (Kinny and Friend, 1997), but there is no *apparent* evidence of metamorphism *at* ca. 2780 Ma. This led Friend and Kinny (2001) to suggest that the Assynt and Rhiconich Terranes were separate Archaean crustal blocks of differing age and early history that were only finally juxtaposed by a major episode of shearing during the along the Laxfordian Shear Zone at ca. 1750 Ma (Fig. 1). This seems consistent with the apparent absence of ca. 2250 Ma quartz-pyrite veins in the Rhiconich Terrane. However, recent fieldwork and dating by Goodenough et al. (2010; 2013) has found evidence that the Laxford Shear Zone initially formed as an Inverian structure, pre-dating the intrusion of a regional suite of arc-related granitic sheets ca. 1880 Ma into both the Assynt and Rhiconich Terranes. These granites are then overprinted by the main Laxfordian deformation and associated amphibolite-facies metamorphism, which ranges from 1790-1670 Ma (Corfu et al., 1994; Kinny and Friend, 1997; Love et al., 2010). In this case the absence of the quartz-pyrite veins to the north of the Laxford Shear Zone is perhaps consistent with significant Laxfordian-age reactivation leading to final juxtaposition of the two terranes.

97. Conclusions

Formatted: Font: Italic

Formatted: Font: Italic

1
2
3 558 A hitherto unrecognised set of quartz-pyrite veins have been identified in the Assynt and
4
5 559 Gruinard terranes of the Lewisian complex. The veins consistently cross-cut Badcallian and
6
7 560 Inverian structures in the gneisses, as well as (at least) the majority of Scourie dykes. They
8
9 561 are reworked during Laxfordian shearing events and are also cross cut by a range of later
10
11 562 brittle faulting events. The dominant strike direction of the quartz-pyrite veins suggests
12
13 563 emplacement during a regional NW-SE extension of the crust, whilst sulphur isotope
14 564 analyses of the pyrites ~~suggest are consistent with~~ a primitive mantle origin for the fluids.
15

16 565 The Re-Os date of 2249 ± 77 Ma for the pyrite within the veins is consistent with the
17
18 566 field relationships and other known geochronological constraints in the Lewisian Complex.
19
20 567 Both the Scourie dykes and quartz-pyrite veins are most likely developed as Mode I tensile
21
22 568 fractures, but their almost orthogonal present day orientations suggests that whilst the dykes
23
24 569 were emplaced during two or more periods of NE-SW crustal extension and associated
25 570 mafic magmatism ca. 1900-2400 Ma, the quartz-pyrite mineralization ca. 2250 Ma occurred
26
27 571 during an intervening phase of NW-SE extension.

Formatted: Font: Italic

Formatted: Font: Italic

28
29 572 The presence of the quartz-pyrite veins in both the Assynt and Gruinard terranes
30
31 573 confirms their amalgamation prior to ca. 2250 Ma, most likely during the Inverian. The
32
33 574 apparent absence of the veins in the Rhiconich Terrane suggests it may not have been
34
35 575 finally amalgamated with the Assynt and Gruinard terranes until the Laxfordian. More
36
37 576 generally, this study demonstrates the potential value of the Re-Os technique as a means of
38
39 577 dating sulphide mineralisation events in continental basement terrains worldwide.
40
41 578

Formatted: Font: Italic

41 579 **Acknowledgements**

42 580
43 581 This research was supported, in part, by a student grant from the Geological Society of
44
45 582 London to RV. Rob Strachan, an anonymous reviewer and Randy Parrish are-is thanked for
46
47 583 their constructive comments and suggestions ~~on earlier versions of this manuscript~~
48
49 584 reviewers.
50
51 585

52 586 **References**

53
54
55
56
57
58
59
60
61
62
63
64
65

- 1
2
3 587 Attfeld, P., 1987. The structural history of the Canisp Shear Zone, *In: Park, R.G. & Tarney, J. (eds), The early Precambrian rocks of Scotland and related rocks of Greenland*,
4 588 Department of Geology, Keele, 165-174.
5 589
6 590
7 591 Beach, A., 1976. The interrelations of fluid transport, deformation, geochemistry and heat
8 592 flow in early Proterozoic shear zones in the Lewisian complex, *Philosophical Transactions*
9 593 *Royal Society London A*, **280**, 569-604.
10 594
11 595 Beacom, L.E., 1999. *The Kinematic Evolution of Reactivated and Non-Reactivated Faults in*
12 596 *Basement Rocks, NW Scotland*, Unpublished PhD thesis, Queens University, Belfast.
13 597
14 598 Beacom, L.E., Holdsworth, R.E., McCaffrey, K.J.W. & Anderson, T.B., 2001. A quantitative
15 599 study of the influence of pre-existing compositional and fabric heterogeneities upon fracture-
16 600 zone development during basement reaction, *In: Holdsworth, R.E., Strachan, R.A.,*
17 601 *Magloughlin, J.F. & Knipe, R.J. (eds). The Nature and Tectonic Significance of Fault Zone*
18 602 *Weakening*, Geological Society Special Publications, London, **186**, 195-211.
19 603
20 604 Berthé, D., Choukroune, P., and Jegouzo, P., 1979. Orthogneiss, mylonite and non coaxial
21 605 deformation of granites: the example of the South Armorican shear zone. *Journal of*
22 606 *Structural Geology*, **1**, 31-43
23 607
24 608 Cameron, E.M., 1994. Depletion of gold and LILE in the lower crust: Lewisian Complex,
25 609 Scotland, *Journal of the Geological Society*, **151**, 747-754.
26 610
27 611 Cartwright, I. & Valley, J.W. 1991. Low-¹⁸O Scourie dike magmas from the Lewisian
28 612 complex, northwestern Scotland. *Geology* **19**, 578-581.
29 613
30 614 Chapman, H.J. 1979. 2,390 Myr Rb-Sr whole-rock age for the Scourie dykes of north-west
31 615 Scotland. *Nature*, **277**, 642-3.
32 616
33 617 Chattopadhyay, A., Holdsworth, R.E., McCaffrey, K.J.W. & Wilson, R.W. 2010. Recording
34 618 and Analyzing Geospatially Accurate Structural Data through 'Digital Mapping' Technique: A
35 619 Case Study from the Canisp Shear Zone, NW Scotland. *Journal of the Geological Society of*
36 620 *India*, **75**, 43-59.
37 621
38 622 Cohen, A.S., Waters, F.G., O'Nions, R.K. & O'Hara, M.J., 1988. A precise crystallisation age
39 623 for the Scourie Dykes, and a new chronology for crustal development in north-west Scotland.
40 624 *Chemical Geology*, **70**, 19.
41 625
42 626 Coleman, M.L. & Moore, M.P., 1978. Direct Reduction of Sulfates to Sulfur Dioxide for
43 627 Isotopic Analysis, *Analytical Chemical Society*, **50**, 1594-1595.
44 628
45 629 Corfu, F., Heaman, L.M. & Rogers, G. 1994: Polymetamorphic evolution of the Lewisian
46 630 complex, NW Scotland, as recorded by U-Pb isotopic compositions of zircon, titanite and
47 631 rutile. *Contributions to Mineralogy and Petrology*, **117**, 215-228.
48 632
49 633 Coward, M.P. & Park, R.G., 1987. The role of mid-crustal shear zones in the Early
50 634 Proterozoic evolution of the Lewisian, *In: Park, R.G. & Tarney, J. (eds), Evolution of the*
51 635 *Lewisian and Comparable Precambrian High Grade Terrains*, Geological Society Special
52 636 Publications, London, **27**, 127-138.
53 637
54 638 Craig, H., 1957. Isotopic standards for carbon and oxygen and correction factors for mass-
55 639 spectrometric analysis of carbon dioxide, *Geochimica et Cosmochimica*, **12**, 133-149.
56 640
57
58
59
60
61
62
63
64
65

- 1
2
3 641 | Davies, J.H.F.L. & Heaman, L.M., 2014³, New U-Pb baddeleyite and zircon ages for the
4 642 Scourie dyke swarm: A long-lived large igneous province with implications for the
5 643 | Paleoproterozoic evolution of NW Scotland. *Precambrian Research*, [In Press, in review](#).
6 644
7 645 Dickinson, B.B. & Watson, J., 1976. Variations in crustal level and geothermal gradient
8 646 during the evolution of the Lewisian Complex of Northwest Scotland, *Precambrian Research*,
9 647 **3**, 363-374.
10 648
11 649 Droop, G.T.R., Fernandes, L.A.D. & Shaw, S., 1989. Laxfordian metamorphic conditions of
12 650 the Palaeoproterozoic Loch Maree Group, Lewisian Complex, NW Scotland, *Scottish*
13 651 *Journal of Geology*, **35**, 31-50.
14 652
15 653 Finlay, A. J., Selby, D., Osborne, M., 2011. Re-Os geochronology and fingerprinting of
16 654 United Kingdom Atlantic Margin oil: Temporal Implications for regional petroleum systems,
17 655 *Geology*, **39**, 475-478.
18 656
19 657 Friend, C.R.L. & Kinny, P.D. 1995. New evidence for the protolith ages of Lewisian
20 658 granulites, northwest Scotland. *Geology*, **23**, 1027–1030.
21 659
22 660 Friend, C.R.L. & Kinny, P.D. 2001. A reappraisal of the Lewisian Gneiss Complex:
23 661 geochronological evidence for its tectonic assembly from disparate terranes in the
24 662 Proterozoic, *Contribution to Mineralogy and Petrology*, **142**, 198-218.
25 663
26 664 ~~Floyd, P.A., Winchester, J.A. & Park, R.G., 1989. Geochemistry and Tectonic Setting of~~
27 665 ~~Lewisian Clastic Metasediments from the Early Proterozoic Loch Maree Group of Gairloch,~~
28 666 ~~NW Scotland, *Precambrian Research*, **45**, 203-214.~~
29 667
30 668 Goodenough, K.M., Park, R.G., Krabbendam, M., Myers, J.S., Wheeler, J., Loughlin, S.,
31 669 Crowley, Q., L.F.C.R., Beach, A., Kinny, P.D., Graham, R., 2010. The Laxford Shear Zone:
32 670 an end-Archaean terrane boundary? In: Law, R., Butler, R.W.H., Holdsworth, R.E.,
33 671 Krabbendam, M., Strachan, R. (eds.), *Continental Tectonics and Mountain Building*.
34 672 Geological Society Special Publication, **335**, 103-120.
35 673
36 674 Goodenough, K.M., Crowley, Q.G., Krabbendam, M. & Parry, S.E. 2013. New U-Pb age
37 675 constraints for the Laxford Shear Zone, NW Scotland: Evidence for tectono-magmatic
38 676 processes associated with the formation of a Palaeoproterozoic supercontinent.
39 677 *Precambrian Research*, **233**, 1-19.
40 678
41 679 Gramlich, J.W., Murphy, T.J., Garner, E.L. & Shields, W.R., 1973. Absolute isotopic
42 680 abundance ratio and atomic weight of a reference sample of rhenium, *Journal of Research*
43 681 *of the National Bureau of Standards*, **77A**, 691–698.
44 682
45 683 Hamilton, P.J., Evensen, N.M., O'Nions, R.K., Tarney, J., 1979. Sm-Nd systematics of
46 684 Lewisian gneisses: implications for the origin of granulites. *Nature*, **277**, 25–28.
47 685
48 686 Heaman, L.M. & Tarney, J., 1989. U-Pb baddeleyite ages for the Scourie dyke swarm,
49 687 Scotland: evidence for two distinct intrusion events, *Nature*, **340**, 705-708.
50 688
51 689 ~~Hirth, G. & Tullis, J., 1992. Dislocation creep regimes in quartz aggregates, *Journal of*~~
52 690 ~~*Structural Geology*, **14**, 145-159.~~
53 691
54 692 Jensen, L.N., 1984. Quartz microfabric of the Laxfordian Canisp Shear Zone, NW Scotland,
55 693 *Journal of Structural Geology*, **6**, 293-302.
56 694
57
58
59
60
61
62
63
64
65

- 1
2
3 695 Kinny, P., Friend, C., 1997. U-Pb isotopic evidence for the accretion of different crustal
4 696 blocks to form the Lewisian Complex of Northwest Scotland. *Contributions to Mineralogy and*
5 697 *Petrology*, **129**, 326–340.
6 698
7 699 Kinny, P.D., Friend, C.R.L. & Love, G.L., 2005. Proposal for a terrane-based nomenclature
8 700 for the Lewisian Gneiss Complex of NW Scotland, *Journal of the Geological Society*, **162**,
9 701 175-186.
10 702
11 703 Love, G.J.L, Kinny, P.D. & Friend, C.R.L., 2004. Timing of magmatism and metamorphism in
12 704 the Gruinard Bay area of the Lewisian Gneiss Complex: comparisons with the Assynt
13 705 Terrane and implications for terrane accretion, *Contributions to Mineralogy and Petrology*,
14 706 **146**, 620-636.
15 707
16 708 Love, G.J., Friend, C.R.L., Kinny, P.D., 2010. Palaeoproterozoic terrane assembly in the
17 709 Lewisian Gneiss Complex on the Scottish mainland, south of Gruinard Bay: SHRIMP U–Pb
18 710 zircon evidence. *Precambrian Research*, **183**, 89–111.
19 711
20 712 Ludwig, K.R., 1980, Calculation of uncertainties of U-Pb isotope data: *Earth and Planetary*
21 713 *Science Letters*, **46**, 212–220.
22 714
23 715 Ludwig, K.R., 2003, Isoplot/Ex, version 3: A geochronological toolkit for Microsoft Excel:
24 716 Berkeley, CA, Geochronology Center Berkeley.
25 717
26 718 Moorbath, S., Welke, H., Gale, N., 1969. The significance of lead isotope studies in ancient,
27 719 high-grade metamorphic basement complexes, as exemplified by the Lewisian rocks of
28 720 Northwest Scotland. *Earth and Planetary Science Letters*, **6**, 245–256.
29 721
30 722 Morelli, R.M., Creaser, R.A., Selby, D., Kontak, D.J. and Horne, R.J., 2005, Rhenium-
31 723 Osmium arsenopyrite geochronology of Meguma Group gold deposits, Meguma terrane,
32 724 Nova Scotia, Canada: Evidence for multiple gold mineralizing events, *Economic Geology*,
33 725 **100**, 1229–1242.
34 726
35 727 O'Hara, M.J. 1961. Petrology of the Scourie Dyke, Sutherland. *Mineralogical Magazine*, **32**,
36 728 848-865.
37 729
38 730 Park, R.G., 1970. Observations on Lewisian chronology. *Scottish Journal of Geology*, **6**,
39 731 379–399.
40 732
41 733 Park, R.G., 2005. The Lewisian terrane model: a review, *Scottish Journal of Geology*, **41**,
42 734 105-118.
43 735
44 736 Park., R.G. & Tarney, J., 1987. The Lewisian Complex: a typical Precambrian high-grade
45 737 terrane?, In: Park, R.G. & Tarney, J. (eds), *Evolution of the Lewisian and Comparable*
46 738 *Precambrian High Grade Terranes*, Geological Society, London,13-26.
47 739
48 740 [Park, R.G., Cliff, R.A., Fettes, D.J., Stewart A.D., 1994. Precambrian rocks in northwest](#)
49 741 [Scotland west of the Moine Thrust: the Lewisian Complex and the Totridonian. In: W.](#)
50 742 [Gibbons and A.L. Harris \(Editors\), *A Revised Correlation of Precambrian Rocks in the British*](#)
51 743 [Isles. Geological Society of London Special Report, **22**, 6-22.](#)
52 744 [Park et al. 1994.](#)
53 745
54 746 Park, R.G, Tarney, J. & Connelly, J.N., 2001. The Loch Maree Group: Palaeoproterozoic
55 747 subduction-accretion complex in the Lewisian of NW Scotland, *Precambrian Research*, **105**,
56 748 205-226.
57 749
58
59
60
61
62
63
64
65

Formatted: Font: Italic

Formatted: Font: Bold

- 1
2
3 750 Park, R.G., Stewart, A.D. & Wright, D.T. 2002. The Hebridean Terrane. In: Trewin, N.H. (ed)
4 751 *The Geology of Scotland*. Geological Society, London, 45-80.
5 752
6 753 Passchier, C.W. & Trouw, R.A.J., 2005. *Micro-Tectonics*, Springer Berlin Heidelberg, New
7 754 York, 25-66.
8 755
9 756 Peacock, D.C.P. & Mann, A., 2005. Evaluation of the controls on fracturing in reservoir
10 757 rocks, *Journal of Petroleum Geology*, **28**, 385-396.
11 758
12 759 Peacock, D.C.P. & Sanderson, D.J. 1995. Pull-aparts, shear fractures and pressure solution.
13 760 *Tectonophysics*, 241, (1-2), 1-13.
14 761
15 762 Rollinson, H., 1993. *Using Geochemical Data: evaluation, presentation, interpretation*,
16 763 Longman Group UK Ltd, Harlow, 303-306.
17 764
18 765 Selby, D., Kelley, K.D., Hitzman, M.W. & Zieg, J., 2009. Re-Os sulphide (Bornite,
19 766 Chalcopyrite, and Pyrite) systematic of the Carbonate-hosted copper deposits at Ruby
20 767 Creek, Southern Brooks Range, Alaska, *Economic Geology*, **104**, 437-444.
21 768
22 769 Sibson, R.H. 1996. Structural permeability of fluid-driven fault-fracture meshes. *Journal of*
23 770 *Structural Geology*, **18**, 1031-1042.
24 771
25 772 Sheraton, J.W., Tarney, J., Wheatley, T.J. & Wright, A.E., 1973. The structural history of the
26 773 Assynt district, In: Park, R.G. & Tarney, J. (eds), *The early Precambrian rocks of Scotland*
27 774 *and related rocks of Greenland*, Department of Geology, Keele, 13-30.
28 775
29 776 Smoliar, M.I., Walker, R.J., & Morgan, J.W., 1996. Re-Os isotope constraints on the age of
30 777 Group IIA, IIIA, IVA, and IVB iron meteorites, *Science*, **271**, 1099-1102.
31 778
32 779 Snoke, A.W., Tullis, J. and Todd, V.R., 1998. *Fault-related Rocks*. Princeton University
33 780 Press, Princeton New Jersey, New Jersey, 617 pp.
34 781
35 782 Stein, H.J., Morgan, J.W. & Schersten, A., 2000. Re-Os of Low-Level Highly Radiogenic
36 783 (LLHR) Sulphides: The Hurnas Gold Deposit, Southwest Sweden, Records Continental-Scle
37 784 Tectonic Events, *Economic Geology*, **95**, 1657-1671.
38 785
39 786 Stipp, M., Stunitz, H., Heilbronner, R. & Schmid, S.M., 2002. The eastern Tonale fault zone:
40 787 a 'natural laboratory' for crystal plastic deformation of quartz over a temperature range from
41 788 250 to 700°C, *Journal of Structural Geology*, **24**, 1861-1884.
42 789
43 790 Sutton, J. & Watson, J., 1951. The pre-Torridonian metamorphic history of the Loch Torridon
44 791 and Scourie areas in the north-west Highlands, and its bearing on the chronological
45 792 classification of the Lewisian, *Quarterly Journal of the Geological Society*, **106**, 241-307.
46 793
47 794 Tarney, J., 1973. The Scourie dyke suite and the nature of the Inverian event in Assynt, In:
48 795 Park, R.G. & Tarney, J. (eds), *The early Precambrian rocks of Scotland and related rocks of*
49 796 *Greenland*, Department of Geology, Keele, 31-44.
50 797
51 798 Vernon, R.H. 1976. *Metamorphic Processes: Reactions and Microstructure Development*.
52 799 George Allen & Unwin, pp 247.
53 800
54 801 Waters, F.G., Cohen, A.S., O'Nions, R.K. & O'Hara, M.J., 1990. Development of Archaean
55 802 lithosphere deduced from chronology and isotope chemistry of Scourie Dykes, *Earth and*
56 803 *Planetary Science Letters*, **97**, 241-255.
57 804
58
59
60
61
62
63
64
65

1
2
3 805 Wheeler, J., Park, R.G., Rollinson, H.R. & Beach, A., 2010. The Lewisian Complex: insights
4 806 into deep crustal evolution, In: Law, R.D., Butler, R.W., Holdsworth, R.E., Krabbendam, M. &
5 807 Strachan, R.A. (eds), *Continental Tectonics and Mountain Buildings: The Legacy of Peach*
6 808 *and Horne*, Geological Society, London, Special Publications, **335**, 51-79.

7 809
8 810 Wilkinson, J.J. & Wyre, S.L., 2005. Ore-Forming Processes in Irish-Type Carbonate-hosted
9 811 Zn-Pb Deposits: Evidence from Mineralogy, Chemistry, and Isotopic Composition of
10 812 Sulphides at the Lisheen Mine. *Economic Geology*, **100**, 63-86.

11 813
12 814 ~~Wynn, T.J., 1995. Deformation in the mid to lower continental crust: analogues from~~
13 815 ~~Proterozoic shear zones in NW Scotland, In: Coward, M.P. & Ries, A.C. (eds), *Early*~~
14 816 ~~*Precambrian Processes*, Geological Society, London, Special Publications, **95**, 225-241.~~

15 817
15 818 Zhu, X.K., O'Nions, R.K., Belshaw, N.S., Gibb, A.J., 1997. Lewisian crustal history from in
16 819 situ SIMS mineral chronometry and related metamorphic textures. *Chemical Geology*, **136**,
17 820 205-218.

18 821
19 822 **Figure Captions**

20 823
21 824 **Figure 1)** Highly simplified geological map showing the location and orientations of the
22 825 quartz vein clusters (i-vi) studied within the Assynt Terrane of the Lewisian Complex. Note
23 826 that this is not an exhaustive assessment of all quartz veins present in the Assynt Terrane,
24 827 i.e. there may be many more clusters than are shown here. Inset map shows general
25 828 location in Scotland and main Lewisian Complex terranes discussed in this paper.

26 829
27 830 **Figure 2)** Field relationships of quartz-pyrite veins. a) NE-SW vein cross-cutting shallowly-
28 831 NW-dipping Badcallian foliation near Clashnessie (NC 0855 3102). Note offset of layers
29 832 across vein indicating Mode I tensile opening (arrows); b) NE-SW vein (below hammer)
30 833 cross-cutting steep NW-SE Inverian foliation in Canisp Shear Zone (NC 0521 2593); c) NE-
31 834 SW vein cross-cutting Scourie dyke on the shore of Loch Assynt (NC 2135 2510); d) NW-SE
32 835 vein folded and reworked by Laxfordian fabrics, Canisp Shear Zone (NC 0515 2620); e) NE-
33 836 SW vein cut and offset 10cm by NW-SE sinistral brittle fault in Badcallian gneisses close to
34 837 the trace of the Loch Assynt Fault (NC 2110 2517); f) En echelon tensile fractures filled with
35 838 epidote indicating sinistral shear in Badcallian gneisses close to the trace of the Loch Assynt
36 839 Fault (NC 2110 2517); g) ENE-WSW vein with en-echelon off-shoots, indicating a small
37 840 component of sinistral shear parallel to the vein margins (NC 2135 2510); h) Large pyrite
38 841 cluster within a quartz vein (NC1038 2249). Note fracturing of pyrite and characteristic iron

1
2
3 841 oxide staining.
4

5
6 842 **Figure 3)** Orientation data for the regional quartz-pyrite vein suite. a) i) Rose diagram of vein
7 843 trends for the entire Assynt Terrane (for locality-based versions, see Fig. 1), ii) lower
8
9 844 hemisphere equal-area stereoplot of veins with lineated margins; b) Equal area stereoplots
10
11 845 of gneiss foliations (i-iii) and of associated veins from each locality (iv-vi) grouped according
12
13 846 to the inferred age of the wall rock fabric; c) Equal area stereoplots of quartz vein clusters
14
15 847 measured in the six localities (i-vi) shown in Fig 1.
16

17 848 **Figure 4)** Representative microstructures of quartz-pyrite veins viewed using optical
18
19 849 microscope and FESEM. a) Chess-board extinction in large quartz crystals from vein cutting
20
21 850 Badcallian gneisses at Kylesku; b) New grains forming along grain boundaries and
22
23 851 deformation lamellae, reflecting slightly lower temperature overprint in vein located close to
24
25 852 the trace of the Loch Assynt Fault; c) Development of new grains at triple junction grain
26
27 853 boundaries overprinting higher temperature deformation features in vein cutting Inverian
28 854 fabrics near Lochinver; d) Recrystallised S-C fabric in highly sheared veing from the
29
30 855 Laxfordian central part of the Canisp Shear Zone, e) Quartz intergrown with within blocky
31
32 856 pyrite cluster; f) Intricate intergrowths of pyrite and quartz from vein cutting Scourie dyke at
33
34 857 Loch Assynt; g) BSEM image of smooth pyrite (light grey) intergrown with quartz (dark grey)
35
36 858 from the same sample as f). The radial fibrous material is iron oxide replacing pyrite; h)
37 859 Alteration of pyrite (bright grey) along fractures to iron oxides (darker mottled greys), Sample
38
39 860 64.1 (see text for details). Note that all the optical micrographs are cross-polar views.
40

41 861
42
43 862 **Figure 5)** Re-Os data for the pyrite from the quartz-pyrite veins. A) $^{187}\text{Re}/^{188}\text{Os}$ and
44
45 863 $^{187}\text{Os}/^{188}\text{Os}$ plot for all samples and all samples minus sample 64.1; B) ^{187}Re vs $^{187}\text{Os}^r$ plot,
46
47 864 with the $^{187}\text{Os}^r$ data calculated using an initial of 3 ± 13 ; C) Weighted average of Re-Os
48 865 model ages, with the model ages calculated using an initial of 3 ± 13 . See text for
49
50 866 discussion.
51

52 867 |
53

54
55
56
57
58
59
60
61
62
63
64
65

1
2
3
4
5
6
7
8
9
10
11
12
13
14
15
16
17
18
19
20
21
22
23
24
25
26
27
28
29
30
31
32
33
34
35
36
37
38
39
40
41
42
43
44
45
46
47
48
49
50
51
52
53
54
55
56
57
58
59
60
61
62
63
64
65

Figure 6) The chronology of events during the Archaean to Proterozoic in the Assynt Terrane, showing the range of possible Scourie dyke episodes and the vein emplacement period ascertained during the present study.

Table Caption

Table 1) Re-Os and S isotope data for pyrite from quartz veins in the Lewisian Complex, NW Scotland. All uncertainties are reported at the 2s level, $^{187}\text{Os}/^{188}\text{Os}$ uncertainties reported at 2SE; all data are blank corrected, blanks for Re and Os were 2.7 ± 1.1 and 0.40 ± 0.42 pg, respectively, with an average $^{187}\text{Os}/^{188}\text{Os}$ value of 0.37 ± 0.17 (1SD, $n = 2$). All uncertainties are determined through the full propagation of uncertainties of the Re and Os mass spectrometer measurements, blank abundances and isotopic compositions, spike calibrations, and reproducibility of standard Re and Os isotopic values. $^{187}\text{Os}_r$ presented are calculated using initial $^{187}\text{Os}/^{188}\text{Os}$, plus its uncertainty, from regression of data using $^{187}\text{Re}/^{188}\text{Os}$ vs. $^{187}\text{Os}/^{188}\text{Os}$ isochron plot; rho is the error correlation.

1 = $^{187}\text{Os}_r$ determined from an initial $^{187}\text{Os}/^{188}\text{Os}$ of 0.9 ± 9.0 (Fig. 5A).

2 = $^{187}\text{Os}_r$ determined from an initial $^{187}\text{Os}/^{188}\text{Os}$ of 3 ± 13 (Fig. 5A). With the exception of sample RO297-3/28, the calculated % $^{187}\text{Os}_r$ is very similar using either initial $^{187}\text{Os}/^{188}\text{Os}$ values of 0.9 ± 9.0 or 3 ± 13 . For sample RO297-3/28 the % $^{187}\text{Os}_r$ decreases to ~72.8% using an initial $^{187}\text{Os}/^{188}\text{Os}$ value of 3 ± 13 . A model age can be directly calculated using

$$^{187}\text{Os}_r/^{187}\text{Re} = e^{t\lambda} - 1$$

3 = Model age determined using an initial $^{187}\text{Os}/^{188}\text{Os}$ value of 0.9 ± 9.0 (Fig. 5A).

4 = Model age determined using an initial $^{187}\text{Os}/^{188}\text{Os}$ value of 3 ± 13 (Fig. 5A).

5 = The reproducibility based on full replicate analyses of internal laboratory standards was ± 0.2 per mil (1σ).

Formatted: Superscript

Formatted: Superscript

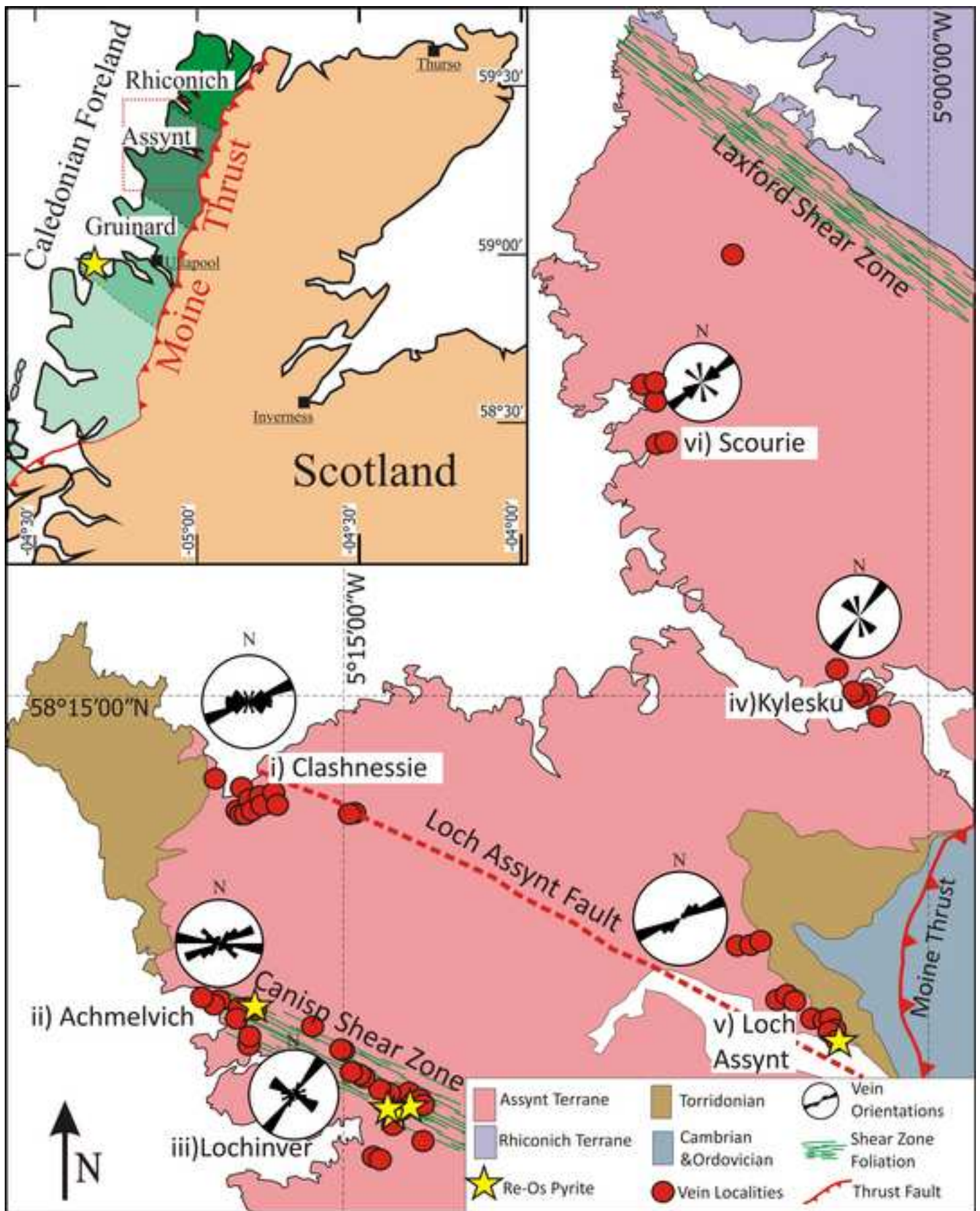
Formatted: Superscript

Formatted: Superscript

Table 1: Re-Os and S isotope data for pyrite from quartz veins in the Lewisian Complex, NW Scotland.

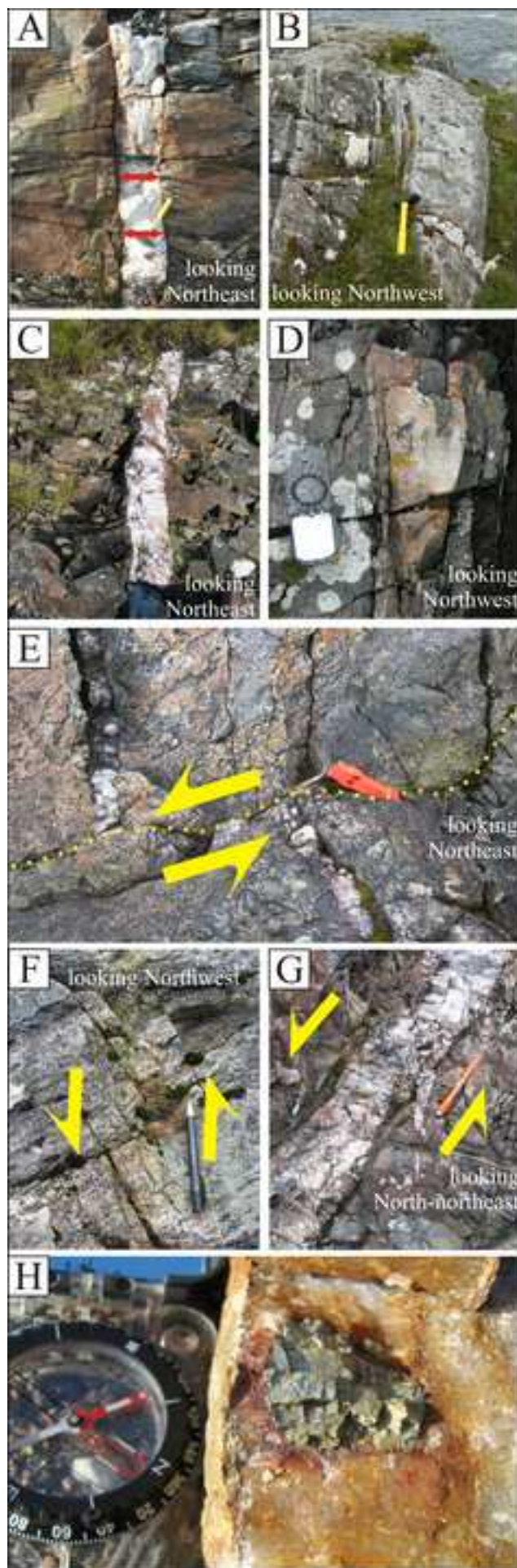
Batch/Sample	Location (Lat/Long) / OS	Re (ppb) total	±	Os (ppt) total	±	$^{187}\text{Re}/^{188}\text{Os}$	±	$^{187}\text{Os}/^{188}\text{Os}$	±	rho	^{187}Re (ppb)	±	$^{187}\text{Os}^f$ (ppt) ¹	±	$^{187}\text{Os}^f$ (ppt) ²	±	% $^{187}\text{Os}^f$	Model age ³	±	Model age ⁴	±	$d^{34}\text{S}$ (‰) ⁵
<i>Gcinard Bay</i>																						
RO297-2/G-Bay	57°51.567' N / 005° 27.121' W 8310, 7817	25.2	0.1	602.1	45.1	12670.5	627.9	473.6	27.4	0.851	15.86	0.06	591.6	21.1	589.0	24.1	99.8	2198.5	78.9	2189.0	90.1	3.0
<i>Lochan Sgeireach</i>																						
RO297-3/28	58°10.640' N / 005°16.374'W 0755, 2560	6.8	0.0	298.8	26.9	265.6	21.2	11.04	1.4	0.636	4.27	0.02	163.1	145.7	129.3	209.8	91.8 - 72.8	2249.4	2010.2	1790.5	2904.7	1.1
<i>Waterworks</i>																						
RO297.5/64.1	58°09.049' N / 005°13.357' W 1038, 2249	8.0	0.0	242.8	33.9	395.1	49.5	11.56	2.2	0.663	5.02	0.02	135.5	116.3			92.2	1597.6	1371.2			-2.2
<i>Lochniver</i>																						
RO143-1/BH2	58°09.599' N / 005°13.530'W	25.8	0.1	660.5	23.3	4762.4	123.4	186.3	4.9	0.963	16.22	0.06	631.7	30.9	624.6	44.4	99.5	2293.0	112.5	2267.5	161.6	1.9
RO143-4/BH5	58°09.599' N / 005°13.530'W 1012, 2366	23.8	0.1	623.8	20.0	4041.8	96.9	160.8	3.8	0.974	14.98	0.06	592.5	33.4	584.7	48.2	99.4	2328.7	131.7	2298.7	189.8	1.8
<i>Loch Assynt</i>																						
RO194-2/LA2	58°10.703' N / 005°02.471' W 2050, 2540	14.6	0.1	358.2	49.4	17531.0	1729.3	675.2	66.6	0.998	9.19	0.04	353.8	5.0	352.7	7.0	99.8	2265.5	32.9	2258.6	45.7	0.9

Figure
[Click here to download high resolution image](#)



Figure

[Click here to download high resolution image](#)



Figure

[Click here to download high resolution image](#)

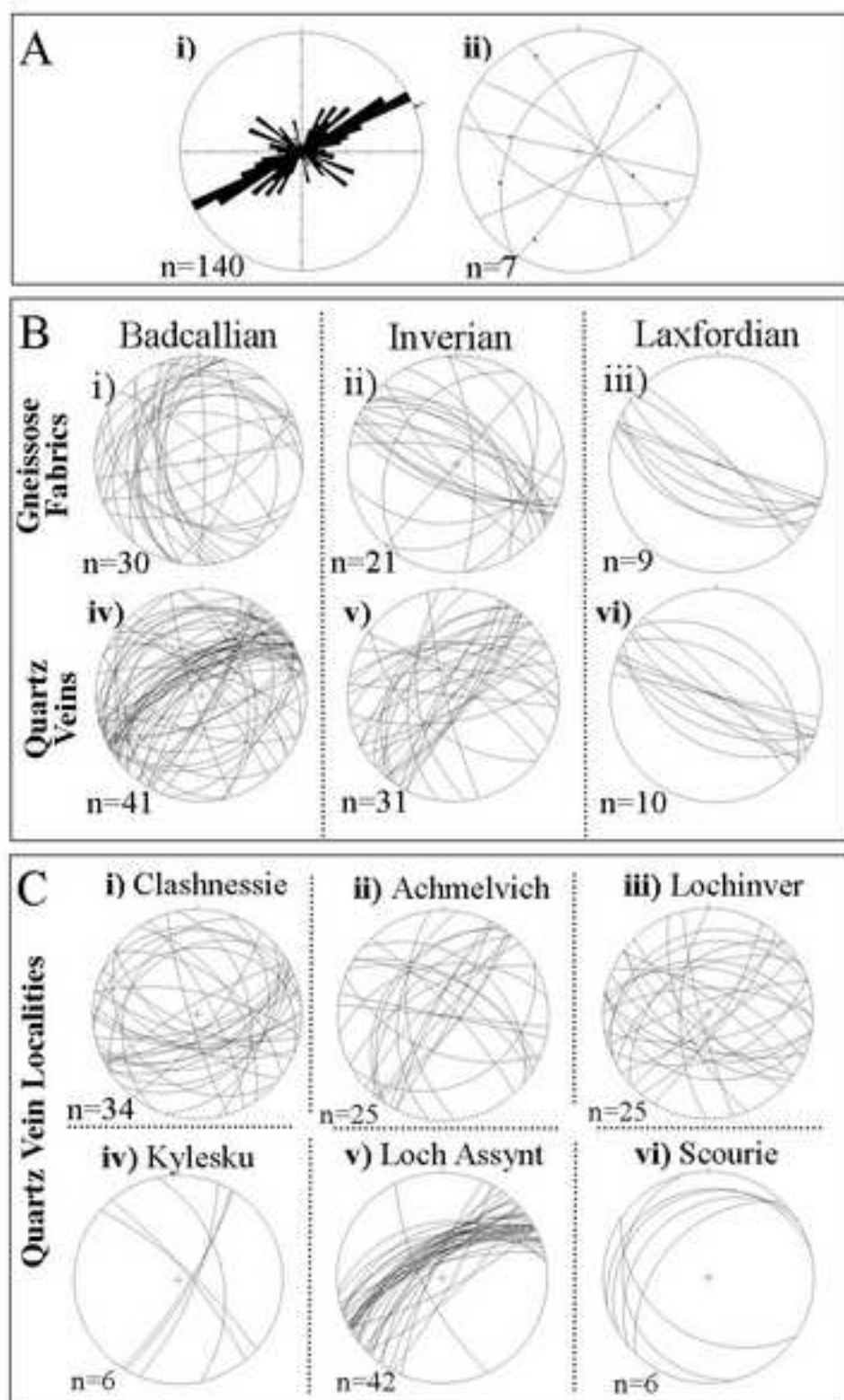
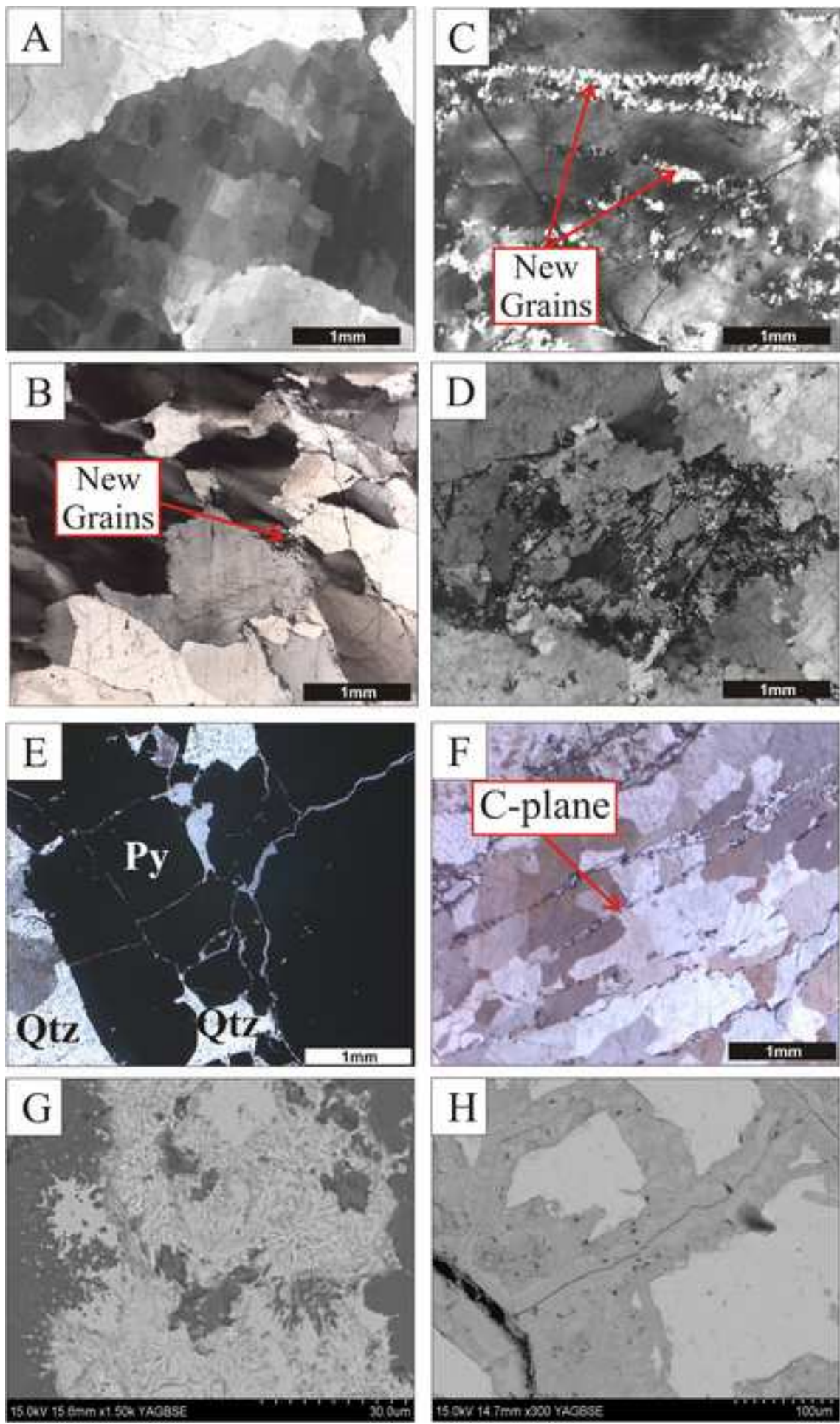


Figure
[Click here to download high resolution image](#)



Figure

[Click here to download high resolution image](#)

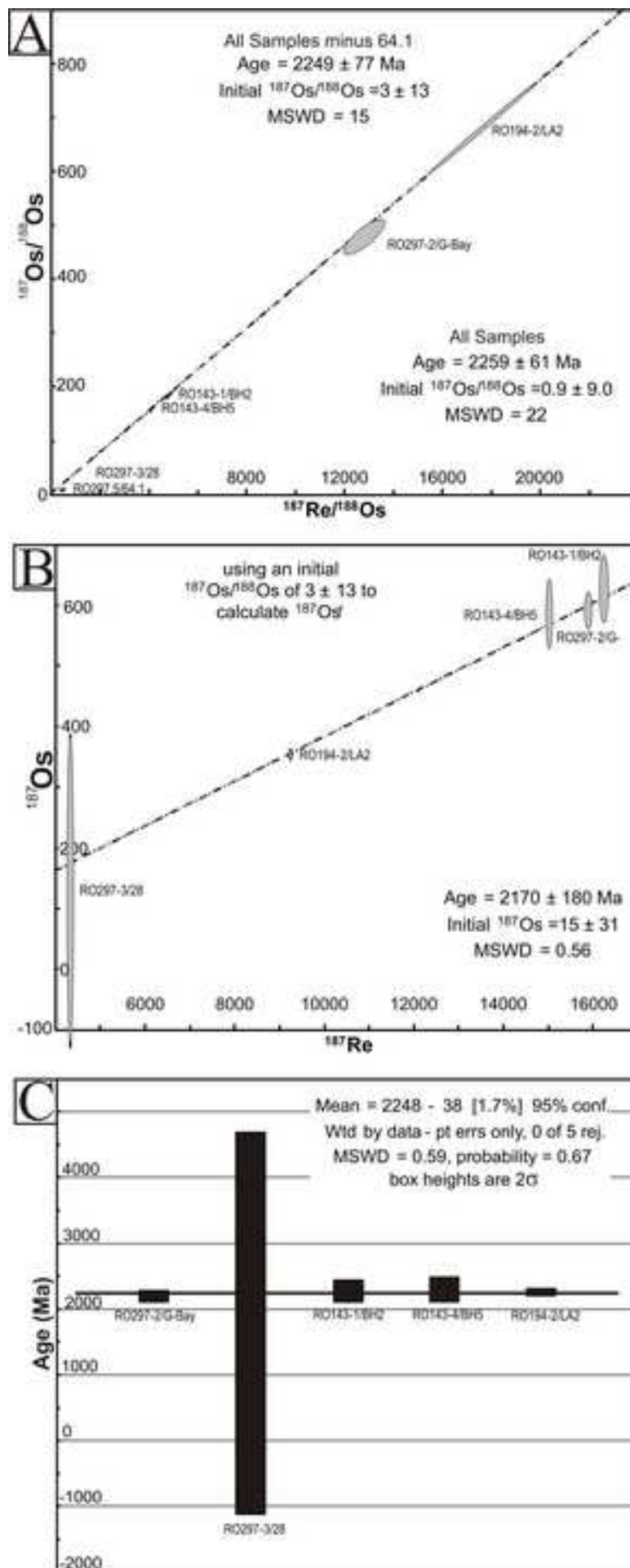


Figure
[Click here to download high resolution image](#)

